Spring 5-11-2015

Neural Basis of Social and Perceptual Decision-making in Humans

Bidhan Lamichhane

NEURAL BASIS OF SOCIAL AND PERCEPTUAL DECISION-MAKING IN HUMANS

by

BIDHAN LAMICHHANE

Under the Direction of Mukesh Dhamala, PhD

ABSTRACT

We make decisions in every moment of our lives. How the brain forms those decisions has been an active topic of inquiry in the field of brain science in recent years. In this dissertation, I discuss our recent neuroimaging studies in trying to uncover the functional architecture of the human brain during social and perceptual decision-making processes.

Our decisions in social context vary tremendously with many factors including emotion, reward, social norms, treatments from others, cooperation, and dependence to others. We studied the neural basis of social decision-making processes with a functional magnetic resonance imaging (fMRI) experiment using three economic exchange games with undercompensating,

nearly equal, and overcompensating offers. Refusals of undercompensating offers recruited the right dorsolateral prefrontal cortex (dlPFC). Accepting of overcompensating offers recruited the brain reward pathway consisting of the caudate, the cingulate cortex, and the thalamus. Protesting of decisions activated the network consisting of the right dlPFC, the left ventrolateral prefrontal cortex, and midbrain in the substantia nigra. These findings suggested that social decisions are the results of coordination between evaluated fairness norms, self-interest, and reward.

In the topic of perceptual decision-making, we contributed to answering how diverse cortical structures are involved in relaying and processing of sensory information to make a sense of environment around us. We conducted two fMRI experiments. In the first experiment, we used an audio-visual (AV) synchrony and asynchrony perceptual categorization task. In the second experiment, we used a face-house categorization task. Stimuli in the second experiment included three levels of noise in face and house images. In AV, we investigated the effective connectivity within the salience network consisting of the anterior insulae and anterior cingulate cortex. In face-house, we discovered that the BOLD activity in the dlPFC, the bidirectional connectivity between the fusiform face area (FFA) and the parahippocampal place area (PPA), and the feedforward connectivity from these regions to the dlPFC increased with the noise level – thus with difficulty of decision-making. These results support that the FFA-PPA-dlPFC network plays an important role for relaying and integrating competing sensory information to arrive at perceptual decisions of face and house.

INDEX WORDS: Functional magnetic resonance imaging (fMRI), Unfairness, Perceptual decision, Social decision, Task difficulty, Dorsolateral prefrontal cortex (dlPFC), Salience network (SN).

NEURAL BASIS OF SOCIAL AND PERCEPTUAL DECISION-MAKING IN HUMANS

by

BIDHAN LAMICHHANE

A Dissertation Submitted in Partial Fulfillment of the Requirements for the Degree of

Doctor of Philosophy

in the College of Arts and Sciences

Georgia State University

2015

NEURAL BASIS OF SOCIAL AND PERCEPTUAL DECISION-MAKING IN HUMANS

by

BIDHAN LAMICHHANE

Committee Chair: Mukesh Dhamala

Committee: Vadym Apalkov

Sarah F. Brosnan

Gennady Cymbalyuk

A.G. Unil Perera

Brian D. Thoms

Electronic Version Approved:

Office of Graduate Studies

College of Arts and Sciences

Georgia State University

May 2015

DEDICATION

Dedicated to my respected parents, my lovely wife Sharada, dear sons Bishal and Bipul, dear brother Bidur and his family

ACKNOWLEDGEMENTS

I feel that I can't thank enough all the wonderful people I had the opportunity to work with during my graduate studies here at Georgia State University (GSU). First and foremost, I would like to express my deepest gratitude to Dr. Mukesh Dhamala for providing me an excellent environment for doing the research of my choice. I will always be indebted to him for his outstanding supervision, under which I was able to make significant scientific contributions while completing my PhD. I would like to thank Dr. Sarah Brosnan, who I had the pleasure to interact with for the social decision-making project, for her scientific guidance, encouragement, and support.

I would also like to thank our collaborators and the committee members. A big thanks goes out to all the wonderful people in Dr. Dhamala's neurophysics research laboratory with whom I have worked, discussed scientific problems, had a fun time, and a wonderful memorable experience here at GSU.

Besides the work place, I would never be able to finish my dissertation without the support of my family. I would like to thank them all, but I know only a word of gratitude is not enough for their tremendous emotional support and encouragement. Special thanks goes to my parents who have been supportive in all aspects of my life. Without their love and support, I would never have been able to come this far. Thanks to my little ones at home who always provide me a good laugh after a hectic and busy day at school. Last, but not the least, heartfelt thanks to my wife, Sharada, who has been always there cheering me up and standing by me through the ups and downs of my life.

TABLE OF CONTENTS

LIST OF TABLES

LIST OF FIGURES

LIST OF ABBREVIATIONS

INS(s)	Anterior insula(e)
AV	Audio and visual
BPA	Bayesian parameter averaging
BOLD	Blood oxygenation level dependent
dACC	Dorsal anterior cingulate
dlPFC	Dorsolateral prefrontal cortex
DCM	Dynamical causal modeling
EPI	Echo-planar imaging
TE	Echo time
FDG	Fixed decision game
fMRI	Functional magnetic resonance imaging
FFA	Fusiform face area
GLM	General linear model
GC	Granger causality
IG	Impunity game
IPL	Inferior parietal lobe
MRI	Magnetic resonance imaging
MT	Middle temporal cortex

MNI	Montreal neurological institute
LOC	Lateral occipital cortex
OC	Overcompensation/(ed)
PPA	Parahippocampal place area
PSS	Point of subjective simultaneity
ROI(s)	Region(s) of interest
SN	Salience network
S1	Somatosensory cortex
SOA	Stimulus onset asynchrony
STN	Substantia nigra
ΔT	Temporal lag
TMS	Transcranial magnetic stimulation
RT	Response time
UG	Ultimatum game
vlPFC	Ventrolateral prefrontal cortex
VT	Ventral temporal cortex

1 INTRODUCTION

1.1 Overview

Decision-making is a highly complex cognitive process and involves the integration and interpretation of available information. The integration of required information for a decision to be made could be either from the highly complex social environment where we live in or from the availability of information in the environment. In either case, the decision-making process produces a final choice that may or may not prompt action. The decision results from interaction of the complex external factors (for example, socio-economic conditions of the decision maker in the social domain, the availability of sensory information in the perceptual domain) and the neural architecture comprised of a highly complex and interconnected circuitry. This dissertation describes three studies we conducted in an attempt to understand the neural mechanisms of decision-making in healthy human participants. The study of the decision-making process from healthy individuals is important not only for the basic understanding of the underlying brain mechanisms, but also to lay the foundations for the study of patients suffering from mental illnesses and neurological disorders whose brain circuitry for decision-making is impaired.

We live in a highly complex social environment surrounded by family, friends, and various cultural and socio-economic conditions. Our everyday decisions and the choices that we make in the context of social interaction, social decisions, have great social values as the decisions not only affect ourselves but also the others in our society. We humans are distinct from other organisms in such decision-making, as many of our decisions are not only based on the basic "animal" needs (e.g., hunger, reproduction) but on social (e.g. fair and unfair), moral (e.g., love, trust, respect, cooperation), and economic values. The complexity of the social decision process varies tremendously with other factors such as intention, punishment, emotions,

risk, and uncertainty. For example, many of our social decisions are influenced by the behavior of others {for review [1-3]}. Similarly, the perception of an object or an event in our environment is based on the available the sensory evidence. The decision, which is based on the gathered sensory evidence, perceptual decision**,** may be affected by various factors such as the ambiguity of sensory information or attention.

Neuroimaging techniques offer the promise of unlocking the mystery of brain processes underlying many cognitive phenomena, including decision-making. We used functional magnetic resonance imaging (fMRI) to describe the brain states that resulted from the neural computation of available information in real-world situations, such as choosing personal benefits versus social norms and categorization of objects in the visual world. In the following chapters of this dissertation, I will discuss the brain mechanisms for such complex and strategic human behaviors and the brain responses of social and perceptual decision-making processes.

1.2 Study of social decision-making

The social decision-making process in humans has been studied for a long time in the laboratory setting to understand details of the neural substrate of the decision-making process and its cognitive aspects. Modern neuroscientific technologies (fMRI, EEG) combined with the theoretical framework from behavioral economics and cognitive psychology allows neuroscientists to study how humans interact with the environment to produce economic behavior. Behavioral economic games provide a useful foundation and well-specified models for the study of the decision-making process in a complex social environment, and they are being used as a tool to establish connections between variables derived from observed behavior with the neuronal data. Thus neuroeconomics, the combination of economics, psychology, and neuroscience, has been making headway on gaining a more detailed picture of the social

decision-making process and greatly extending our knowledge of the brain mechanisms involved in social decision-making, such as the feelings of reward and emotional response to unfair treatment.

In typical economic games, the players are assumed to act rationally in order to maximize their earnings. But, the decision drastically varies with factors like rewards, punishment, emotions, value to social norms, risk, and uncertainty, and different brain areas are recruited to process the information [1-7]. Also, when people actually play these games, they rarely play according to this strategy [8]. In reality, decision-makers are typically both less selfish and more willing to consider factors such as reciprocity and equity than the classical model predicts. The ultimatum game (UG), introduced by W. Guth and colleagues [9], is one of the games used to shed light on reasons for rejections of unfair offers. From a game-theoretic perspective, the responder should accept any non-zero offers. However, humans significantly diverge from this strategy: the offers in the range from 40–60% are usually accepted and below 20% are rejected almost half the time [8]. There are some interesting differences in more traditional cultures [10], but in general, the probability of rejection increases substantially as offers decrease in magnitude. This decision to reject offers in UG has puzzled economists because if people are motivated purely by self-interest, the responder should accept any offer; thus it seems that material self-interest is not the sole motivation of all human beings. These predictive failures of the self-interest model gave rise to the development of social preference models.

A “ social preference ” is now considered to be a characteristic of an individual’s behavior or motives, indicating that the individual cares positively or negatively about others’ material payoff or wellbeing. Thus, a social preference means that the individual’s motives are other-regarding – that is, the individual takes the welfare of other individuals into account. There

is now a large body of experimental evidence in economics and psychology [7,8,11] indicating that a substantial percentage of people are motivated by other regarding preferences.

Another study in UG by Xiao and Houser [12] found that, compared with standard ultimatum games where the only action that responders can take is to accept or reject offers, responders are significantly less likely to reject the unfair offers when they can write a message to the proposers. In particular, proposers' offers of $4 (20% of the total surplus) or less are rejected 60% of the time in standard ultimatum games. When responders can express emotions, only 32% reject unfair offers, and this difference is statistically significant. This study suggested that the desire to express negative emotions can itself become an important motivation underlying costly punishment. Moreover, in impunity game (IG), unlike in UG, the responder can neither punish an unfair proposer nor restore fairness, yet despite this rejection of unfair offers is often observed in experimental studies of the impunity game [13]. Thus the standard explanation of rejection behavior in the ultimatum game, that is, social preferences of inequity aversion and reciprocity [7,11,14], cannot explain the rejection of unfair offers in the impunity game. Thus, previous studies suggested that the neither the role of emotion nor fairness and reciprocity can be ignored in social interactions.

The most complex and advanced brain mechanisms of social decision making processes is influenced by various factors including emotion, reward, and fairness norms. The understanding of such brain process is becoming a target of neuroscientists. Many in the field have attempted to understand the neural correlates of human social behavior, however almost all of these considered only one aspect of inequity: how individuals respond when inequity does not favor them [15-17]. Inequity has, however, two sides: the responder may be over-benefitted (or over-compensated, advantageous inequity), or under-benefitted (or under-compensated,

disadvantageous inequity). One of the goals of this dissertation is to use both inequity condition in the UG and IG and uncover the mystery of the brain processes of those sorts of inequity. How does the brain internalize the preference? Importantly, including both UG and IG permitted us to explore the role of dorsolateral prefrontal cortex when unfairness is perceived in economic exchange. In both UG and IG, rejecting monetary offered affect responder's outcome, however, a new game, the Fixed Decision Game (FDG), was used where protest (rejection to an offer) did not affect the player's earnings. The hypothesis in the new game was that if one values fairness; one would protest more frequently in the FDG unfair conditions, a response that may not appear in other games due to the high cost of doing so. In brain activations, the contrasts of primary interest were between the neural responses to unfair offers as compared to fair offers and the brain network for protesting unfair offers. The details of social decision-making study will be discussed in chapter 2 of this dissertation.

1.3 Study of perceptual decision-making

The neural correlates of perceptual decision-making have been extensively studied in humans and in monkeys in laboratory setting using a simple perceptual discrimination task with two or more forced-choice alternatives [18,19]. It is believed that the brain has to integrate and interpret sensory information to form a decision. Diverse cortical structures are known to be involved in relaying and processing of sensory information available to our sensory system in order to make a sense of the environment around us.

Making sure of the identity of visual or other sensory events is difficult in the case of scantly or briefly available sensory information. For example, when you see a yellow light while driving, you have two options, to stop at or cross the intersection; and your decision to do that will be affected by how far you are from the intersection and your current speed. The decision-

making in yellow light condition compared to the red light (in which case you will have to stop) might be relatively harder as the brain has to integrate all the information in this situation. However, little is known about how such perception and decision is achieved in the brain, translated to motor command, and how the task difficulty modulates the brain response.

Recent findings suggested that anterior insulae (INSs) and the dorsal anterior cingulate cortex (dACC) are a part of the salience network (SN), a key network known to be involved in decision-making and thought, also to be important for the coordination of behavioral responses [20-27]. However, how these nodes in SN contribute to the decision-making process from segregation of stimuli to the generation of an appropriate behavioral response remains unknown. We aimed to contribute to answering this question using audio and visual synchrony and asynchrony perception task (AV). The details of functional architecture of SN in perceptual decision-making task will be discussed in chapter 3 of this dissertation.

Out of many secrets of human brain function is how information is processed in order to reach a decision and which brain areas are involved in these kinds of perceptual decision-making processes, both of which are widely investigated questions in the field of neuroscience [18-20,28-36]. The answers for such questions were investigated with the brain responses of varying degrees of sensory evidence available to our sensory system. Various paradigms have been developed, including vibrotactile frequency discrimination [28], visual motion discrimination [37], and face-house discrimination [38] under conditions of different intensity of sensory information conditions. These studies suggested that the decision-forming process for such simple perceptual decision-making tasks starts off with the integration of sensory evidence for each choice by lower-level sensory neurons [28,37,38]. For example, faces and houses categories were represented in ventral temporal areas namely fusiform face areas (FFA) and

parahippocampal place area (PPA) [35,39,40] and the decision is then thought to be computed in higher-order cortical regions by comparing the difference in amount of sensory information for each choice [19,38]. But it remains to understand how the decision is computed and where.

In this dissertation, I will discuss one of our experiments that examines the neural correlates of perceptual decision-making in human brain and clarifies the relationship between sensory representations in a lower order sensory cortex and decision-making hub, the dorsolateral prefrontal cortex. The innovation in this study is that we varied the difficulty level of tasks and studied the relationship between the category responsive visual areas and higher order areas with different difficulty levels. We further established a causal link between FFA, PPA, and dlPFC in perceptual performance.

Our findings challenge some of the previous findings in perceptual decision-making studies. We provided the evidence that a perceptual decision of faces and houses results from the neural interaction between category responsive visual processing area in ventral temporal cortex (VT) and the higher cortical area in dorsolateral prefrontal cortex (dlPFC). We argued that the increase in blood oxygen level dependent (BOLD) response in the dlPFC with task difficulty in perceptual decision making task is the consequence of decision related-processes, which challenges the highly publicized previous study of observed deactivation [38]. Their study [38] predicted that regions involved in decision-making would be more active on trials with less noise. In chapter 4, I will discuss and summarize how perceptual decisions of faces and houses, the result from the neural interactions between the visual and prefrontal cortices.

1.4 Selected scientific contributions during my PhD program

Some of my scientific contributions during my PhD are listed below. The dissertation is based upon the first three works in the list.

- **B. Lamichhane** and M. Dhamala, "Perceptual decision-making difficulty modulates feedforward effective connectivity to the dorsolateral prefrontal cortex", (submitted)
- **B. Lamichhane** and M. Dhamala, "The salience network and its functional architecture in a perceptual decision: an effective connectivity study", (Brain Connectivity, doi: 10.1089/brain.2014.0282, 2015).
- **B. Lamichhane**, B. M. Adhikari, S. F. Brosnan and M. Dhamala, "The Neural Basis of Perceived Unfairness in Economic Exchanges", Brain Connectivity, 4(8): 619-30 (2014).
- B. M. Adhikari, K. Sathian, C. M. Epstein, **B. Lamichhane** and M. Dhamala, "Oscillatory Activity in Neocortical Networks during Tactile Discrimination near the Limit of Spatial Acuity", Neuroimage, 91, 300-310 (2014).
- S. Bajaj, **B. Lamichhane**, B. M. Adhikari and M. Dhamala, "Amygdala Mediated Connectivity in Perceptual Decision-making of Emotional Facial Expressions" Brain Connectivity, 3(4), 386-397 (2013).
- B. M. Adhikari, E. Goshorn, **B. Lamichhane**, and M. Dhamala, "Temporal order judgment of audiovisual events involves network activity between parietal and prefrontal cortices", Brain Connectivity 3(5), 536-545 (2013).
- **B. Lamichhane**, B. M. Adhikari, M. Dhamala "Functional role of human anterior insulae in perceptual decisions: consistent findings and unanswered questions" (to be submitted)
- **B. Lamichhane** and M. Dhamala, "Salience network and task dependent functional architecture of its nodes in human perceptual decision-making" (to be submitted).

2 THE NEURAL BASIS OF PERCEIVED UNFAIRNESS IN ECONOMIC EXCHANGE

2.1 Introduction

Our sense of fairness helps us to regulate our lives in society. Our perception of inequity leads to a range of emotions [41-44] and often motivates us to react negatively [6,9,45], even when we know that such a reaction may lead to a personal cost [45]. Such negative reactions have been observed to varying degrees across diverse cultures [10], and nonhuman animals share a similar trait [46], indicating a strong biological predisposition. Human social decision-making in situations of inequity is often viewed as a competition between the norms of fairness and self-interest [5,47]. Thus, deviations from self-interested behavior leading to reciprocal fairness are hypothesized to reflect our values for social norms and inequity aversion [11]. This notion of social decision-making as a result of competition between sense of fairness and self-interest is primarily based on the studies of human responses in the two-person (proposer and responder) economic exchange by using only one aspect of inequity, how individuals respond when inequity does not favor them [15-17]. Inequity has, however, two sides: the responder may be over-benefitted (or over-compensated, which is advantageous inequity) or under-benefitted (or undercompensated, which is disadvantageous inequity). Is there an asymmetry in our responses and, hence, in our sense of fairness between these two inequity conditions? If yes, what are the brain mechanisms underlying this difference? To what degree do reactions depend on whether the responder's actions can influence the players' outcomes, and what are the differences in brain mechanisms for protests as compared to refusals? This study addresses these questions using functional neuroimaging techniques in three two-person economic exchange games: the Ultimatum Game (UG), the Impunity Game (UG) and a new Fixed Decision Game (FDG).

The UG is the game most commonly used to determine how people make decisions in situations of inequity [9]. In the UG, the first player, the proposer, splits a sum of money with the second player, the responder. If the responder accepts the offer, both participants are rewarded accordingly, while if the responder rejects the offer, neither player receives any money. Thus a refusal by the responder leads to him or her receiving absolutely less, but relatively the same as, the partner. The responder's rejection in the UG has been interpreted as a way by which he or she punishes the unfair proposer and/or signals to the proposer (or others) that the unfair treatment has occurred. A variant of the UG is the Impunity Game (IG: [48]). The IG is procedurally identical to the UG, except that the responder's rejection response affects only his or her own payoff, and not the proposer's. Unlike in the UG, in the IG, the responder cannot punish an unfair proposer, nor does a refusal result in equality. In fact, a refusal results in both an absolutely and relatively less good outcome for the responder. Nonetheless, responders still refuse, possibly due to frustration or to reinforce their commitment to fairness [13]. Finally, we were interested in how responders would use a 'protest' option that did not change either the proposer's or the responder's outcome. Thus we developed a new game, the Fixed Decision Game (FDG), a variation on the UG and IG. In the FDG, a distribution of offers was shown to the responder, who could choose to either protest or not protest these decided outcome offers, but in neither case were the outcomes to either player altered. Additionally, in contrast to the UG, in the FDG there is no competition between economic self-interest and fairness norms, particularly in the case of overcompensation, because the responder still gets the designated monetary amount even if he or she protests a decision.

Fairness-related social decisions are known to be motivated by self-interest, self-versus-other comparisons and fairness norms[5,9]. Neuroimaging studies have shown that such

decisions activate several brain regions: the insula, dorsolateral prefrontal cortex (dlPFC) and the anterior cingulate cortex (ACC) for the perception of unfair offers [3], the ventral striatum for fair offers [49], and the ventromedial prefrontal cortex and caudate for social rewards [50]. The competition between self-interest and fairness norms [9,47] is neutrally instantiated in the right dorsolateral prefrontal cortex (dlPFC), where activity is found to be associated with undercompensating (low unfair) offers [3,47]. The dlPFC is believed to play a role in limiting the selfish motive and implementing fairness [3]. Disruption of the right, but not the left dlPFC (using repetitive transcranial magnetic simulation; [47]) substantially reduces participants' willingness to reject their partners' unfair offers. However, the right dlPFC is also found to be recruited when responders decide whether or not to punish a partner in a two party economic exchange by rejecting an unfair economic deal proposed by that partner. Thus, the precise role of the dlPFC in these refusals is still debated; evidence supports both inhibition of self-interest [47] and punishment of norm violators [3,51]. We hypothesized that, if the role of the dlPFC is to inhibit the self-interest, dlPFC activity would be elevated in the UG and IG rejection where the self-interested motivation is suppressed, but not necessarily the FDG game, in which a protest does not influence outcomes. If the dlPFC has a role in punishing the norm violators, dlPFC activity should be higher in the UG than in the IG or FDG when responders are rejecting undercompensating offers.

One limitation of the previous fairness-related studies is that they primarily consider only one aspect of inequity - disadvantageous inequity, or participants' reactions when they received less than a partner. Inequity aversion includes two components, both disadvantageous inequity aversion and advantageous inequity aversion, or an aversion to outcomes that overly benefit the individual as compared to a partner [7]. In the current study, we included overcompensated

offers. First, this allowed us to explore whether individuals would refuse rewards in order to bring about equity when they are overcompensated with respect to a partner. Second, we explored whether undercompensated and overcompensated offers equally triggered the disapproval response [3,45]. One of our main foci was to determine the brain mechanism that differentiates between these two conditions. Third, we explored whether individuals would protest more frequently in the FDG condition, where the protest does not affect their earnings, which may allow them to appear to be 'nicer' people without paying any cost to do so. This could potentially uncover situations in which people have a taste for fairness, but one that does not appear in traditional games due to the high cost of being fair (e.g., conflict between their taste for equity and their self-interest in their own material outcomes).

We hypothesized that there would be a low rejection rate for overcompensated offers, which is in line with previous behavioral studies [52,53]. For the associated brain response, we hypothesized that the activity would be different between overcompensated and undercompensated offers, and between overcompensated and fair offers. The manifested behavioral outcome in overcompensated offers might be triggered by feelings similar to those experienced for being rewarded, which would invoke the brains' reward circuitry [54-60]. We additionally predicted that there would be a higher protest rate in the FDG than the refusal rate in the UG. We hypothesized that the brain activity would differ between the protested decisions and not protested decisions, allowing us to learn about the brain mechanisms of protesting decisions [61]. Here, we predicted that protesting a decision would involve the brain network that coordinates between the inner speech of subjective feeling and protest [62,63] and social norm compliance [64].

2.2 Materials and Methods

2.2.1 Participants

Eighteen people (10 males and 8 females; age: 25.2 ± 6.2 years (mean ± standard deviation)) participated in the experiment. A pre-scanning written interview was conducted. Participants were asked to fill an interview form with a number of questions related to MRI safety and medical history. All of our participants reported that they were right-handed and had normal or corrected-to-normal vision, no history of medical, psychiatric, or neurological diagnoses, and were not taking any medication. A written informed consent was obtained from each participant before the experiment according to the procedures approved by the Institutional Review Board of Georgia State University.

2.2.2 Experimental task

We used two established economics games, the Ultimatum and Impunity games, and included a new game, which we called the Fixed Decision Game (FDG). In all of these games, there were three offer distributions: fair, unfair-low (e.g., disadvantageous to the participant), and unfair-overcompensated (e.g., advantageous to the participant). The distributions were from by the random splits of $100 in above mention three contexts as: fair offers ($40 < offer < $60), unfair low (undercompensated) offers ($0 < offer < $20), and unfair high (overcompensated) offers ($80 < offer < $100) in all three games. There were thus nine offer conditions (three games type × three offer conditions), but during testing only one offer condition at a time was presented in the computer screen (Figure 2.1). Offer conditions were randomized across the session. Presentation (Neurobehavioral systems, http://www.neurobs.com) was used to display the offers to the participants and to record participants' behavioral responses.

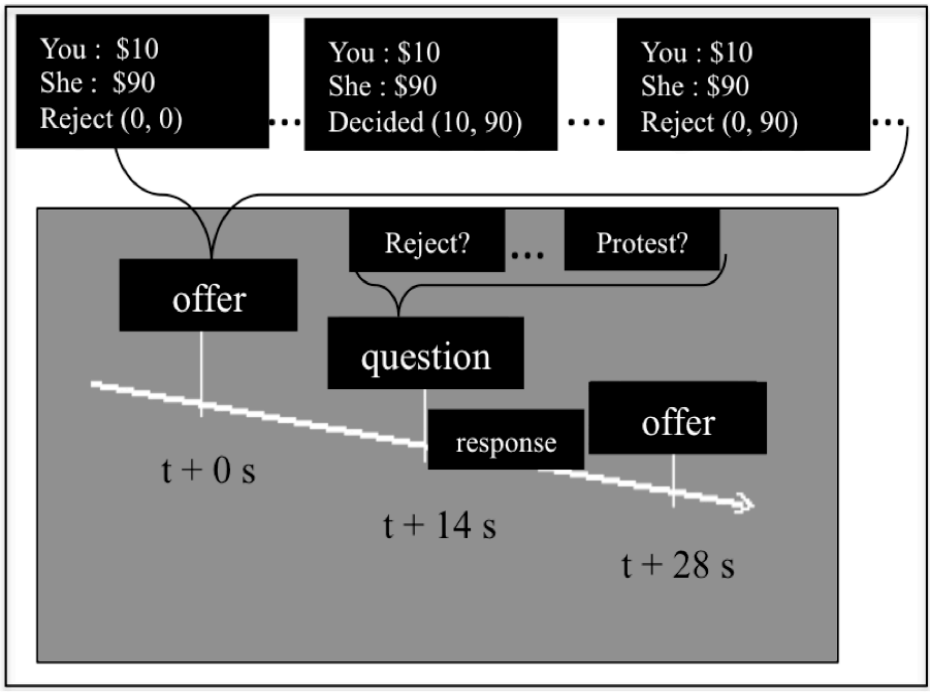

Figure 2.1 Task paradigm.
A single round of the economic games consisted of the proposer's offer, the question and the responder's yes or no choice. The time interval between an offer and a question was 14 seconds. Offers, along with the game outcomes should the offer be rejected, were displayed for 4 seconds on a computer-projected screen. Here, in three sample offers, participants saw both the offer and the payoffs to both parties should they reject the offer. Regarding the latter, "Reject (0,0)" means that if the offer is rejected, $0 will go to the responder and the proposer (this is ultimatum game, UG); "Reject (0, 90)" means $0 to the responder and $90 to the proposer (impunity game, IG); "Decided (10, 90)" means a fixed offer of $10 to the responder and $90 to the proposer (fixed decision game, FDG). Responders could indicate their yes or no choices by pressing one of the two buttons on a response box after the question, "Reject?" for the UG or IG and "Protest?" for the FDG, appeared on the screen.

The responder (the participant in our study) could either reject or accept the proposer's offers in the UG and IG, and could choose either to protest or not to protest the fixed offers in the FDG. The outcome of the responder's action varied according to the rules of these games (Table 2.1). The responder's rejection led to no pay-offs to both players in the UG, but only the responder lost their payoff in the IG. In the FDG, the responder could change neither their own nor the partners' outcomes, but could choose to protest the decided offers.

Table 2.1 Economic games and outcomes.

Game	Option	Outcomes for Reject/Protest	
		Proposer	Responder
Ultimatum (UG)	Reject/Accept	$0	$0
Impunity (IG)	Reject/Accept	Offer amount	$0
Fixed Decision (FDG)	Protest/Not Protest	Offer amount	Offer amount

Before scanning, each participant saw the pictures and names of possible players (proposers), who would be referred as 'he' or 'she' in each trial (Figure 2.1). They were also told that they would be playing with real money, and that they would be compensated for a percentage (approx. 2%) of their earnings, up to $50 in total. The participants were told how the games were played and what the possible outcomes of each game were. The participants were asked to practice a few rounds of the task in a computer setup before going into the scanner. In the scanner, each participant played 30 rounds of each of the three games from each of the three distributions discussed above, with games and payoff conditions randomized across the session. This was done in three 860s-long functional runs. Each run had two 10s rest (no task) durations, one in the beginning and the other at the end. Each round (trial) consisted of an offer and the question. The offer and the associated question ("Reject?" or "Protest?") were each displayed for 4 s. The time between the onset of an offer and a question was 14 s. Participants decided whether to reject or not to reject the offers in the between offer-to-question block. The participants were asked to make a response after the question mark (?) appeared on the screen.

2.2.3 Data acquisition and analysis

Participants were scanned on 3-T Siemens fMRI scanner in the Biomedical Imaging Technology Center at Emory University while they played three economic games and decided whether (i) to reject or not to reject unfair (under- or over-compensated) and fair monetary offers (UG and IG), and (ii) to protest or not protest a fixed monetary offers (FDG). The functional scans were acquired with T2*-weighted gradient echo-planar imaging (EPI) sequence (repetition time (TR), 2000 ms; echo time (TE), 32 ms; flip angle, 90°; field of view, 256×256 mm^2; dimensions, 64×64×33; voxel dimensions, 3 mm×3 mm×4 mm). For each of the three functional runs, 430 volume images were taken. Behavioral responses were analyzed using Matlab. The analysis of fMRI images was carried out by using Statistical Parametric Mapping (SPM8, http://*www.fil.ion.ucl.ac.uk/spm/software/spm8*). Slice timing and motion-corrected images were spatially normalized to the Montreal Neurological Institute (MNI) template. The voxels were resized to 3×3×3 mm^3 per voxel resolution. Finally, images were spatially smoothed using an 8-mm FWHM Gaussian Kernel. A random-effect, model-based, univariate statistical analysis was performed in a two-level procedure. At the first level, a separate general linear model (GLM) was specified for 18 task conditions [3 offer types × 3 games × 2 response conditions (that is accepted/not protested and rejected /protested conditions)) for each of decision and response block plus time-courses of 6 motion parameters (as nuisance covariates) were entered in GLM. The individual contrast images of all participants from the first level GLM were then taken into a second level analysis for a separate one-sample t-test. Resulting summary statistical maps were then corrected for multiple comparisons by using AlphaSim command in AFNI [65]. These maps were overlaid on a high-resolution structural image in Montreal Neurological Institute (MNI) orientation.

2.2.4 Behavior data analysis

In all of the games, we used three offer distributions mentioned above: undercompensating, nearly equal and overcompensating. We planned to test whether there was an asymmetry in behavioral responses and, hence, in the sense of fairness between these three conditions. Among games, we were interested in the degree to which the responder's actions could influence the players' outcomes in both undercompensated and overcompensated offer conditions. The rejection or protest rates for three distinct distributions for each game were calculated for individual participants and averaged for the group in each condition. Wilcoxon sum rank tests were performed to compute the significance levels of behavioral differences across conditions.

2.2.5 Functional connectivity analysis

The analysis of functional relationship between the brain regions, the functional connectivity, was done by defining the regions of interests (ROIs). ROIs were defined by generating a sphere of 6 mm radius around the coordinate of local maxima from the group level analysis of fMRI data by using MarsBar [66]. The time courses from all the voxels within each ROI and all participants were extracted from the sets of the ROIs. To investigate the brain mechanism for accepting overcompensated offers and to explore how the brain internalized a overcompensated offer, we contrasted the brain activity of accepting overcompensated offers with that of fair offers [57,60] as "High unfair > fair (UG + IG)". We hypothesized that a network of brain regions involved in reward processing [54-60] would be activated. This was the first set of ROIs. The second set of ROIs was chosen from the group level analysis of contrast " Low unfair protested > fair not protested (in FDG)," to investigate the neural correlated of protesting a decision. Time courses were then segmented into trials for accepting

overcompensated versus fair offers from the first set of ROIs and for protesting versus not protesting the fixed decided undercompensated offers condition from the second set of ROIs. We calculated pairwise correlation coefficients from trial by trial time series between the ROIs of the respective sets. To estimate the average effect, we used Fisher's z-transformation [67-69] on cross-correlation values. The correlation coefficients were converted into their equivalent Fisher's z-values $(z = \arctan h(r))$ to compute average Fisher's z-value. The average Fisher's z-values for each participant and each pair of ROIs were then used to calculate the grand average z-value, the significance level p and the corresponding correlation coefficient. This analysis was done separately for accepting overcompensated offers and fair offers from the first set of ROIs and for protesting and not protesting the fixed decided undercompensated offers from the second set of ROIs.

2.2.6 Directed functional connectivity analysis

We performed Granger causality (GC) analysis to characterize the directional influences between ROIs, as the functional connectivity does not reveal the direction of information flow. We extracted the voxels time courses for each ROI from all participants. Since fMRI-BOLD signals are believed to originate from smoothing of neuronal activity by the HRF [70,71], we constructed hidden neural signals by hemodynamic deconvolution for each ROI as suggested in previous studies [71-75]. We used these deconvolved fMRI-BOLD time series for functional connectivity calculation.The ensemble-mean removed segmented deconvolved time series from separate voxels and participants were treated as trials for reliable estimates of the network measures. We calculated the frequency dependent nonparametric Granger causality spectra [76] for pairs of ROIs, separately for both set of RIOs. From the spectral GC, the time-domain values were obtained by integrating the causality spectra over the entire frequency range. The

significant GC spectra were defined by setting a GC threshold above the random-noise baseline. To compute the threshold value of GC, we constructed a set of surrogates by randomly permuting trials data from each participant and used the random permutation technique [77,78]. The threshold was thus based on the null hypothesis that there was no statistical interdependence between nodes when trials were randomized. We computed GC spectra from all possible pairs of ROIs with 300 random permutations and picked maximum GC on each permutation. By fitting the distribution with gamma-distribution function [76], we obtained the threshold for GC spectra at significance $p < 10^{-3}$ separately from each set of ROIs. This threshold GC was used to identify significantly active directed network activity among three ROIs for both sets of ROIs. We computed the time-domain GC values for significantly active network directions.

2.3 Results

2.3.1 Behavioral Results

Most (88%) of the fair offers were accepted in all games, whereas most of the undercompensated offers were rejected and protested (>80%) in the UG and FDG. While we did not find any difference in the frequency with which undercompensated offers were rejected or protested between the UG and the FDG, the rejection rate of undercompensated offers in the IG was less (39.9%) than that of the UG (z-score = 3.26, $p<0.01$) and than the protestation rate in the FDG (z-score = 3.23, $p <0.01$). The overcompensated offers were not rejected to the same degree as undercompensated ones in any of the three games, including the FDG, where protest was not costly. Participants more frequently rejected or protested the undercompensated offers as compared to the fair offers and overcompensated offers in all games (z-score > 3.3, $p<0.001$ in the UG and FDG; z-score = 2.65, $p<0.01$ in the IG; Figure 2.2 and Table 2.2). They did not

respond differently to the overcompensated conditions as compared to the fair conditions in any of the games (Figure 2.2).

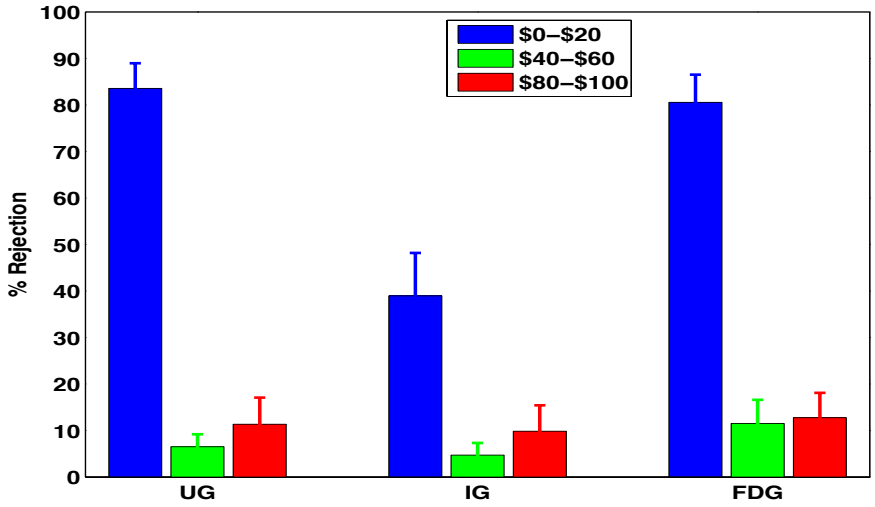

Figure 2.2 Behavioral response.
These are the group averages of rejection or protest rates for three distinct distributions of offers displayed to the responders, $0-$20 (unequal low offers), $40-$60 (nearly equal or equal offers) and $80 - $100 (unequal high offers) out of $100. Each participant played 30 rounds of each game [Ultimatum Game (UG), Impunity Game (IG) and Fixed Decision Game (FDG)) during three fMRI runs. Approximately 2% of the total earnings were given to the participants. Error bars here represent standard errors of the means.

Table 2.2 Behavioral rejection rates in economics games

Games	Choices	Undercompensated offers	Fair offers	Overcompensated offers
UG	Reject	84.5 %	6.5 %	11.3 %
IG	Reject	38.9 %	4.7 %	9.8 %
FDG	Protest	80.6 %	11.5 %	12.8 %

2.3.2 Imaging Results

2.3.2.1 Brain activity associated with undercompensated offers

In order to explore the precise role of the dlPFC in two-person economic exchanges, we contrasted the conditions for undercompensating offers from the UG and IG with FDG as: (i) UG>FDG, (ii) IG>FDG and, (iii) IG>UG. In all of these cases (i - iii), the dlPFC was activated (Figure 2.3 (A-C)) .The details of the brain activations with the multiple comparisons correction is shown in Table 2.3. We also compared the level of activity (% signal change) in the dlPFC for each game during accepting (or not protesting) conditions with rejecting (or protesting) conditions (Figure 2.3 (D-F)). We found that the dlPFC activity was significantly higher ($p<0.05$) when rejecting offers as compared to accepting offers in the UG, IG and in protesting offers compared to not protesting offers in the FDG.

Table 2.3 Brain activations.
All the activations survived a significance threshold at $p < 0.005$ and cluster threshold of $k > 10$. [for AlphaSim corrected (*) $p < 0.05$, (**) $p < 0.001$]

Contrast (Economics Game)	Brain region	Cluster size	Voxel t (z-equivalent)	MNI coordinates
Low UG > low FDG	Right dorsolateral prefrontal cortex (dlPFC)	22**	3.18 (2.79)	30, 47, 28
	R thalamus	14**	3.24 (2.82)	18, -10, 13
Low IG > low FDG	dlPFC	35**	4.75 (3.74)	42, 14, 22
	R inferior temporal cortex	47**	5.26 (4.00)	48, -56, -17
	L cuneus	17	4.19 (3.43)	-12, -70, 4
Low unfair (IG) > Low unfair (UG)	L lingual gyrus	820**	4.21 (3.44)	-15, -67, -2
	L middle temporal gyrus	78**	4.10 (3.37)	-60, -58, -2
	L superior temporal gyrus	19	3.88 (3.24)	-45,14, -23
	dlPFC	30*	3.19 (2.79)	45, 14, 31
	L culmen	23**	3.28 (2.48)	-30, -64, -26
	L fusiform gyrus	78**	3.42 (2.94)	-36, -52, -11
	L thalamus	22**	4.77 (3.75)	-24, -25, -2
High unfair > fair (UG + IG)	R thalamus	26**	4.92 (3.83)	9, -22, 7
	L caudate	12*	4.61 (3.66)	-12, -1, 22
	R cingulate	12*	4.24 (3.46)	18, 2, 31
Low unfair protested > fair not protested (FDG)	dlPFC	10**	3.80 (3.19)	54, 17, 37
	L mid brain	11**	3.57 (3.04)	-6, -22, -20
	L ventrolateral prefrontal cortex (BA 45/47) (vlPFC)	11**	3.44 (2.95)	-48, 17, 4

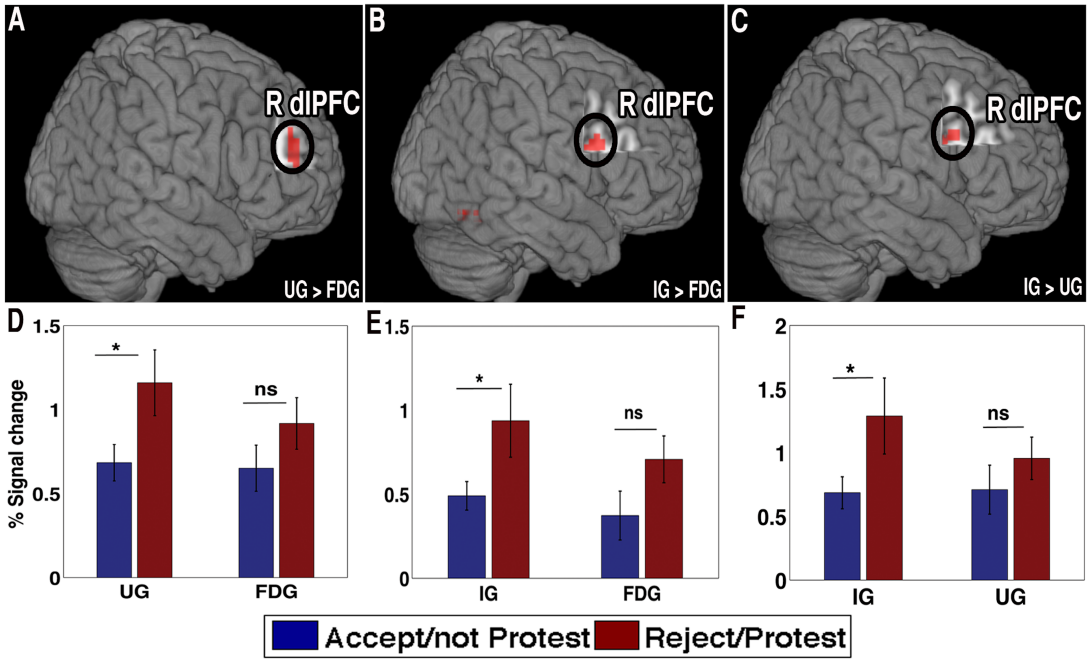

Figure 2.3 Right dorsolateral prefrontal cortex activity.
(A, D) The right dorsolateral prefrontal cortex (dlPFC) showed heightened activity during the rejection of unfair undercompensated offer in the UG as compared to the FDG and corresponding % signal change for rejected/protested and accepted/not protested offers. (B, E) dlPFC activity while rejecting of unfair undercompensated offers in the IG as compared to unfair undercompensated offers in the FDG and % signal change for rejected/protested and accepted or not protested offers. (C, F) dlPFC activity during the rejection of unfair undercompensated offers in the IG as compared to unfair undercompensated offers in the UG and % change for rejected and accepted offers. Here, *: $p<0.05$; ns = not significant.

2.3.2.2 Brain activity associated with overcompensated offers

In order to understand the brain mechanism of accepting overcompensated offers, we contrasted the brain response from overcompensated trials in the UG and IG with that from fair trials [60]. We found significant activation in the left caudate in the dorsal striatum, the right middle cingulate gyrus and the right thalamus when participants decided to accept overcompensated (OC) offers as compared to fair offers (Figure 2.4). Further, the average percent signal changes in these regions differed significantly ($p<0.05$) between the trials when the participants accepted OC offers and the trials when they rejected these offers (Figure 2.4

(C)). Also these regions were found to be functionally connected while accepting the OC offers (Figure 2.4 (A)) but not in accepting the fair offers (Figure 2.4 (B)).

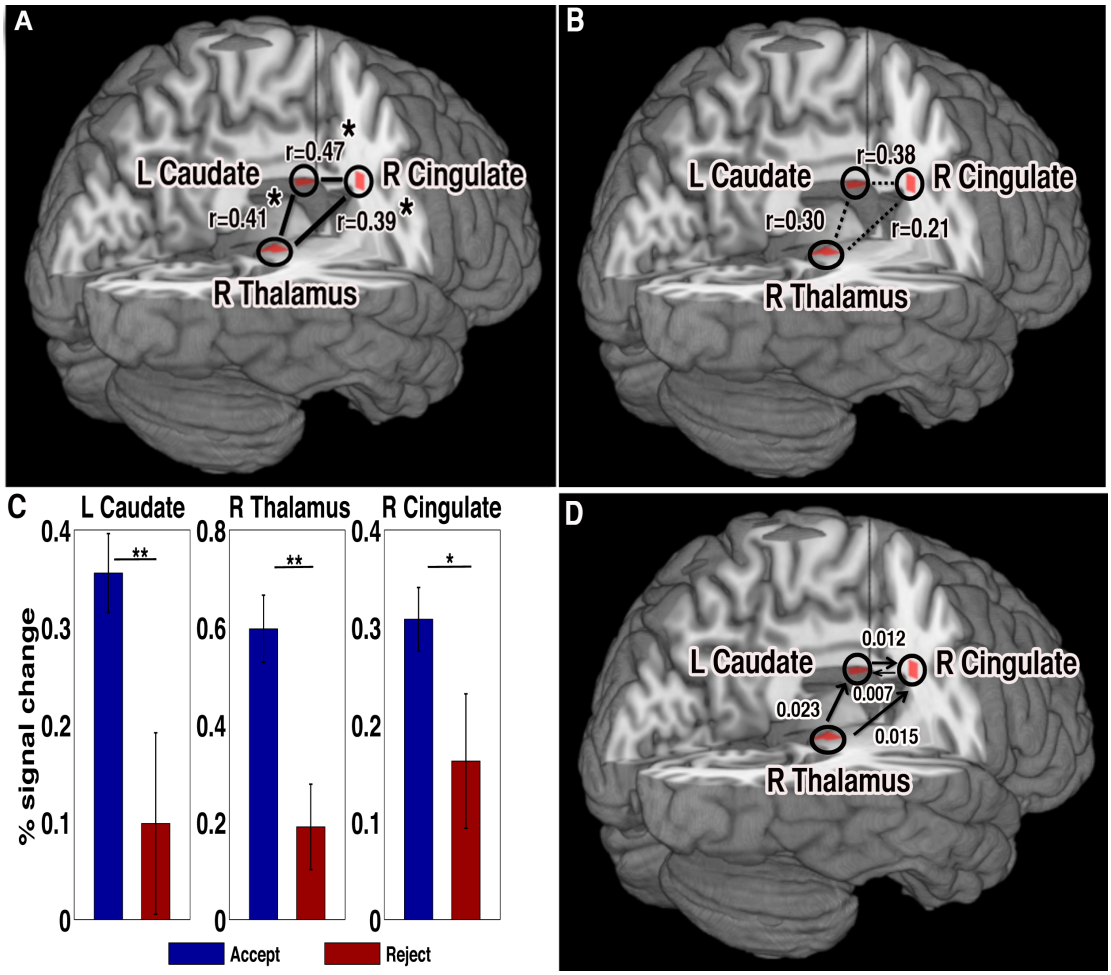

Figure 2.4 Brain node and network activity related to accepting overcompensated offers in the UG and IG.
(A) The left caudate, right thalamus and right cingulate cortex became relatively more active in unfair high offers (overcompensated offers) than in fair offers. This activation analysis included the trials from the UG and IG games. There was significant functional connectivity among these regions during unfair high offer trials. (B) There was not a significant connectivity pattern during fair offers. (C) The average BOLD signal changes in all of these regions were significantly different between the trials when the participants accepted overcompensated offers and the trials when they rejected these offers. (D) The directed functional connectivity pattern is significant at $p<0.001$ (with multiple comparisons corrections). The cingulate cortex receives a dominant information flow from the caudate and thalamus. Here, *: $p<0.05$, **: $p<0.01$.

We obtained the directed functional connectivity within this network based on the hidden neuronal responses derived from the deconvolution of hemodynamic responses (Figure. 2.4 (D)). The Granger causality results showed that thalamus exerted causal influences to both the caudate and the cingulate. There were bidirectional influences between the caudate and the cingulate, but the influence from the caudate to the cingulate was stronger.

2.3.2.3 Brain activity associated with protesting a decision

We isolated the brain areas that were activated when a responder was protesting a decision by contrasting the trials in which he or she protested versus did not protest in the FDG. This allowed us to further elucidate the neural circuitry associated with protesting a decision. Protesting a decision produced significant activation in two structurally [79] and functionally [80] connected brain regions in the left ventrolateral prefrontal cortex (vlPFC) within the inferior frontal gyrus (BA 45/47), the right middle frontal gyrus (dlPFC (BA 9)), a sub-region in the prefrontal cortex, and in the left mid brain in the substantia nigra (STN) (Figure 2.5). These regions vlPFC and dlPFC, dlPFC and STN were found to be functionally connected during protest (Figure 2.5 (A)), but not when individuals chose not to protest (Figure 2.5 (B)). There was bidirectional directed functional connectivity between these pairs of regions; vlPFC and dlPFC; dlPFC and STN. The causal influence was stronger from vlPFC to dlPFC than for the opposite direction. The causal influences were nearly equal in strength from dlPFC to STN and to the opposite direction (Figure 2.5 (C)).

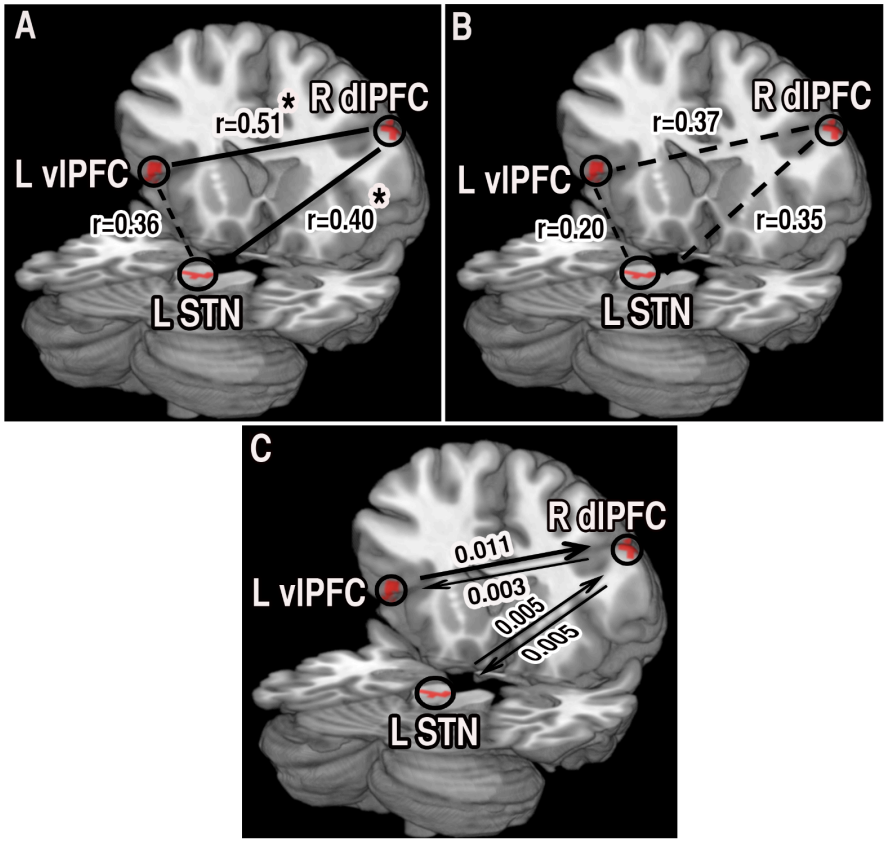

Figure 2.5 Brain node and network activity related to protesting fixed decided offers.

(A) The left substantia nigra (L STN), the right dorsolateral prefrontal cortex (R dlPFC) and the left ventrolateral prefrontal cortex (L vlPFC) became more active during the protest of undercompensated offers than during not protesting fair offers. vlPFC and STN were functionally associated with dlPFC during protest. (B) This functional association was not significant in decided fair offers. (C) Although there were bidirectional network interactions of R dlPFC with L vlPFC and L STN, the R dlPFC received a dominant information flow from L vlPFC during the protest of undercompensated offers.

2.4 Discussion

Primarily based on the Ultimatum Game (UG) and the brain response to disadvantageous inequity, previous neuroimaging studies proposed that human decision-making in the context of unfair offers is a result of competition between cognitive and emotional processes in the brain. In this study, we included both disadvantageous and advantageous inequity conditions to explore

the asymmetry in the sense of fairness (e.g., whether reactions are the same in situations of over- versus under-compensation) and its neural substrates. Our result further showed that a different neural system comes into play in the situations when the responder protests against unfair outcomes without altering these outcomes. Here, we discussed the results of the behavioral responses, fMRI activations and brain networks obtained in three different economic games, the UG, the IG and the FDG.

2.4.1 Behavioral response

In all three games, participants showed their sensitivity to being disadvantaged by refusing or protesting outcomes more often when they were offered less money than a social partner. On the other hand, participants did not show any sensitivity to overcompensation; we found no significant difference in rejection or the protest rate for overcompensated offers as compared to fair offers. These results add to the discussion about the degree to which humans are sensitive to the outcomes of others as compared to themselves. While it is very clear that humans care about others' outcomes [5,14], they are also more interested in their own outcomes than those of others [52] and when sensitivity to others' outcomes may result in a drop in one's own outcome, people prefer not to have that knowledge [53]. Additionally, it is possible that even these prosocial outcomes may be overstated in the case of explicit experimental situations as compared to otherwise similar daily interactions [81]. However, despite disliking being disadvantaged, humans do not uniformly refuse disadvantageous offers [82]. Our results showed that participants were sensitive to how their refusal influenced both their own and their partner's outcomes; participants were less likely to refuse the unequal outcomes in the IG, where refusing resulted to $0 payoff for them but not the partner, than the UG, where refusing resulted to $0 payoff for both participants. This reflects previous work showing that people refuse unequal

outcomes in the IG at about half the frequency for which they refuse the same distribution in the UG [13]. These results from the UG and IG games altogether suggest that the refusals in the UG are not about the punishment to the proposer. Similarly, the refusals in the IG are not an effort to engender equity.

In the UG, there is a tension between acquiring more resources and achieving equity, but in the FDG, individuals could protest such offers without losing resources, presumably dissolving this tension. Thus, we predicted higher protest rates in the FDG than the refusal rate in the UG. Nonetheless, in the FDG, when participants could protest without affecting their material outcomes, participants did not protest with any more frequency than they refused overcompensated outcomes in the IG and UG. That is, despite the essentially non-existent cost of protesting, people frequently chose not to do so. This indicates that participants are not failing to refuse offers in the UG in order to gain resources. One possible explanation for this is that participants were not concerned about the inequity to their partners in the overcompensated conditions. This also extends to disadvantageous offers towards the responder him or herself.

2.4.2 Dorsolateral prefrontal cortex (dlPFC)

The dlPFC is a part of cognitive system that represents goals and the means to achieve them [83,84], and also plays a role in evaluating the fairness-related behaviors and outcomes [85]. In two-person economic exchange games, such as the UG, the dlPFC is usually activated while rejecting undercompensated offers. However, whether its role is to inhibit self interest [47] or to punish the norm violators [3,51] is not resolved yet. Our finding of significantly increased BOLD activity in the dlPFC while participants are rejecting undercompensated offers in the UG (where rejection needs to inhibit economic self interest) as compared to that of the FDG, (where

monetary gain is fixed, meaning no concern about monetary loss and no self-control is required) supports the role of the dlPFC in self-control [86].

To understand its possible role in punishment, we further contrasted the undercompensated offer condition in the IG (where there is no punishment goal) with that of the UG and FDG. We found significantly higher dlPFC activity while rejecting monetary offers in the IG compared to the UG and FDG. Because there is no direct punishment goal associated with rejection in the IG, our results do not support the role of dlPFC for maintaining punishment goals. The higher dlPFC activity while refusing undercompensated offers in the IG might be because it requires a higher level of self-control because refusing in the IG results in both an absolute and a relative loss, while refusing in the UG results only in an absolute loss. The role of the dlPFC in self-control is further supported by a recent study in which disrupting activity in the right dlPFC via transcranial magnetic stimulation (TMS), generated fewer rejections of unfair offers [47]. Moreover, the significant signal change (%) in the dlPFC while rejecting offers as compared to accepting offers in both the UG and IG game conditions suggests that the dlPFC might be involved in inhibiting the appetitive desire for money, which allows individuals to choose socially appropriate options in the implementation of fairness related goal rather than a punitive response to unfair treatment.

2.4.3 Neural correlates of accepting overcompensated offers

Reward plays a major motivational role in changing the behavior of humans and other animals. Our behavioral results clearly showed that people were motivated not to reject or protest overcompensated offers. Importantly, from the brain analysis, the approval response to the overcompensated offers was found to be triggered by the reward related brain circuit consisted of the left caudate, right cingulate gyrus and right thalamus [54-60]. The role of the caudate in

reward processing is further supported by a positive correlation of caudate activation with increased monetary reward [57,59,60]. Similarly, activity in the cingulate gyrus [60] and the thalamus have been found to be associated with rewards [59,60,87,88]. Thus here, too, it is reasonable to argue that the brain might have internalized the overcompensated offers as rewards.

This argument is also supported by the low frequency of protestation of overcompensated offers in the FDG. The low rate of refusals may not be surprising in the IG and UG because responders lose materially by rejecting the offers. However, individuals who possess the taste for fairness should protest when there is no cost to doing so, as in the FDG. The failure to do this may indicate that they do not find these outcomes troubling. This argument is further supported by previous work [89] done by using a two-person economic exchange game (the trust game) in which hemodynamic responses in the caudate were found to be correlated with an increase in trust (that is, an increase in payments to the partner). In the same direction, a study by Hikosaka et al. [54] and single neuron recording in non-human [90-92] have shown that the dorsal striatum is the main hub associated with reward and goal-directed behaviors. The cingulate is known to be involved in conflict monitoring [30,93], and is active when choosing actions associated with reward [94] and in reward related decision making [60,94-96].

Furthermore, the functional connectivity analysis revealed functional connection between them (Figure2.4 (A)) while accepting overcompensated offers, but not in the fair offer condition (Figure 2.4 (B)). The caudate and cingulate were causally influenced from the thalamus and they also communicated when people accepted overcompensating offers (Figure 2.4 (D)). The caudate is well known for processing reward-related information [58,88] and is thought to involve the outputs of the midbrain dopaminergic system [97]. The strong causal influence from

the caudate to the cingulate might be the reward signals, or the incentive motivation, that helps the cingulate resolve conflict [30,93] between social fairness norms and accepting unfair overcompensation offers. This might lead towards the acceptance of unfair overcompensated offers by modifying or changing behavioral responses [95,96]. The significantly higher BOLD signal during the acceptance of overcompensated compared to fair offers (Figure 2.4 (C)) showed the involvement of this brain network towards the acceptance of overcompensating offers. The involvement the caudate-cingulate –thalamus network might be either in the selection of action associated with higher value outcomes [54-56,94] or in the processing of rewards [54,57-60,95,96], and does not support previous thinking that inequity aversion is symmetric in humans [1,9,45,98].

2.4.4 Neural correlates of protesting a fixed decision

The monetary gain in the FDG is fixed and so, unlike in the UG, there is no conflict (or tension) between acquiring monetary gain and promoting (if not achieving) equity when protesting a decision in the FDG. As a result, the act of protesting a decision is based only on the responders' attitudes concerning fairness (e.g., the current reward is uninvolved) [80], which are highly rooted on one's knowledge, awareness, personality traits [99,100] and perception of proposer's intention [17], and require cognitive control [83,86]. The elevated right dlPFC activity while protesting the decision might indicate executive top-down control of such behavior [83,101,102]. This view is further supported by the previous findings [103] that patients with right prefrontal lesions were characterized by the inability to behave in normatively appropriate ways, despite the fact that they were keenly aware of the prevailing norms, such as the fairness norm (in tasks similar to ours; [6]). The higher dlPFC activity while protesting the

undercompensated offers compared with not protested fair offers is also consistent with the previous finding [47] that the dlPFC is involved in social norms enforcement.

However, the dlPFC is not the only region activated when protesting an undercompensated offer; the vlPFC, a region involved in verbal reasoning [104] and inner speech [63], and the STN are coherently activated. The vlPFC has consistently been identified as the neuro-anatomical basis of inner speech and reliably gets activated when participants are asked to silently articulate sentences or single words [62]; dysfunction also disrupts inner speech [63]. In our case, the vlPFC might be feeding (the observed dominant causal flow from the vlPFC to the dlPFC, Figure 2.5(C)) its inner speech of frustration/protestation induced by unfair treatment to the dlPFC while protesting the decision. Further, the strong functional connectivity between the dlPFC and the vlPFC when protesting a decision (Figure 2.5(A)), but not when participants choose not to protest (Figure 2.5(B)), suggests that the interaction between these regions is important during the processing of participants' reaction to unfair offers. The similar connectivity pattern between the right dlPFC and the left ventral prefrontal cortex [105] was observed in rejecting unfair offers. As these brain areas are not yet fully developed in children, adolescents, or even young adults [106], these groups are not fully able to evaluate appropriate social norms [64]. Thus the network formed by these region might be a part of the neural circuitry involved in social norm compliance [64]. Additionally, brain activity in the left STN (midbrain), a reward related brain region [59,97,107], might reflect the pleasure feeling induced by decision of protesting (symbolically) unfair decision [87]. Thus, the evidence suggests that the act of protestation or the expression of frustration [61] resulted from the coordination of neural activity among the dlPFC, vlPFC, and STN and was triggered by the frustration of a social norm violation.

Previous studies on human social decision-making in the context of economic games have shown that there is competition between self-interest and fairness norms, and little is known about the neural basis of resolving such conflict. Here, by using three games, the UG, IG and FDC, we find evidence supporting the role of the right dlPFC in the social decision making process. By including an overcompensated offer condition, we found that, contrary to earlier reports [7,9], people do not make decisions that benefit others at a cost to themselves. Further, accepting overcompensated offers was found to be associated with activity in the brain reward's system [57-60,88]. Finally, we found that the ability to protest without cost does not influence participants' tendency to do so, indicating that the cost involved in refusals is not sufficient to explain the lack of rejections.

Behavioral results in our new FDG were very similar to those typically found in the UG in low unfair condition [3,13], however, the difference in the rate of rejection of overcompensated offers was of the same degree as fair offers in all games. This is surprising, especially in the case of the FDG, because the responder could lodge a protest for a decision to unfair offers without affecting their material outcomes. Future neuroimaging studies on social decision-making processes can examine the interplay between over- and under-compensation, as well as the role of actual rejection versus protest. In particular, this sample space should be extended by investigating similarities and differences due to a variety of factors such as personality traits [99,100], perception of proposer's intention [17], age [108] and culture [10]. Levels of perceived fairness are known to change in certain psychiatric illnesses, such as bipolar disorder and personality disorders [109,110]. This study with fairness related games and neuroimaging probes could provide some basis for future studies of cognitive functions and dysfunctions useful for the diagnosis and understanding of mental disorders.

3 THE SAILENCE NETWORK AND ITS FUNCTIONAL ARCHITECTURE IN A PERCEPTUAL DECISION: AN EFFECTIVE CONNECTIVITY STUDY

3.1 Introduction

The anterior insulae (INSs) are known to be involved in perceptual decision-making independent of response modalities [22,111]. The increase in INSs activity at the moment of a perceptual decision during an image recognition task [112] further supports their role in the decision-making process [113]. Also, INSs have been shown to be involved in the integration of perceptual information in the auditory and visual domains [114,115], and were found to be strongly affected by task difficulty level [116].

Another brain region on the medial wall of the frontal lobe, the dorsal anterior cingulate cortex (dACC), has long been implicated in movement initiation [117,118]. dACC lesions can lead to difficulties initiating complex voluntary movements and actions [119,120]. The activity in dACC is known to have a direct causal role on choosing an action during the goal directed action selection [20,121,122], and is involved in the top-down modulation to primary motor cortex [123].

In task-based functional imaging, INSs and dACC have been found to be co-activated [20,32,112] and are anatomically interconnected [124]. The spike of activity in this network was found time-locked with the ‘‘moment of recognition’’ in a perceptual discrimination task [112]. This is in accordance with the previously documented evidence on their role in the decision-making process [111,125]. The network formed by INSs and dACC has been named the “salience network (SN)” [24,36].

Previous studies have indicated a broad role of SN in the decision-making process, including the implementation of goal-directed tasks [20,21]. However, when available sensory

information is scant, the task of decision-making becomes difficult and is reflected in the uncertainty of the decisions [22,126,127]. For optimal performance of decision-making, the brain has to put together the ambiguous information to arrive at the perceptual decisions [128]. How is the ambiguity resolved? What is the role of the INSs in the ambiguity resolution? How a goal-directed behavior evolves from the causal interactions of nodes within the SN remains to be understood.

In this study, we aimed to understand the contribution of each node of SN in the decision-making process, from segregation of stimuli to response selection. To pursue the goal, we used functional magnetic resonance imaging (fMRI) with dynamical causal modeling (DCM), a technique that infers effective connectivity from fMRI data, coupled with a Bayesian model evidence technique. Thirty-three healthy participants were scanned and asked whether the presented pairs of audio-visual (AV) stimuli were synchronous or asynchronous. Stimuli pairs were presented in blocks of eight pairs with a participant-specific temporal lag (ΔT) between audio and visual stimulus onset. The perception of synchrony or asynchrony is strongly influenced time lag (ΔT). Time spacing between the tone and flash was unique to each individual. The individuals' ΔT was chosen by finding the point of subjective simultaneity (PSS) (details in the methods and materials). The task difficulty, the cognitive demand of our task, was manipulated by creating the temporal lag near the PSS.

3.2 Materials and Methods

3.2.1 Participants

Thirty-three healthy individuals (17 females and 16 males; mean age, 27.54 years) participated in this experiment. All participants had normal hearing and normal or corrected to normal vision, as well as normal neurological history. Participants were compensated for their

participation. The Institutional Review Board (IRB) for Georgia State University and Georgia Institute of Technology, Atlanta, Georgia, USA approved the experimental procedure. All participants provided written informed consent in accordance with institutional guidelines

3.2.2 Stimuli

We used a pair of auditory (a tone) and visual (a flash of light) stimuli. The auditory stimulus consisted of a 440-Hz–30-ms tone, while the visual stimulus consisted of a 30-ms yellow-red flash from the disc of 0.7cm radius. The auditory stimulus was delivered through a pair of earphones, one on each ear, and visual stimulus was flashed at the central position on the computer screen. Sound was presented first with a stimulus onset asynchrony (SOA) depending on the participants' point of subjective simultaneity (PSS) (for details see task and behavioral paradigms). Participants judged whether the pair of stimuli appeared to have been presented simultaneously (synchronously) or not (asynchronously). They were asked to report their decision by pressing the left or the right button on a button box with either their right index or middle finger. Subjects were asked to indicate their decision as quickly and as accurately as possible outside the scanner and after the question mark appeared on the screen in the fMRI run. The trials in which they failed to respond or made an incorrect response were discarded for further analysis. The presentation software (http://www.neurobs.com) was used to display stimuli and to control task trial sequences. Prior to the task, the experimenter explained the instructions and procedure to each participant. Example trials were shown to help make the subjects more familiar with the task procedure.

3.2.3 Task and behavioral paradigms

Outside the fMRI scanner. The experimental task outside the scanner was divided into two separate sessions and each session consisted of a single run. The first session was aimed to

identify a " point of subjective simultaneity (PSS)", i.e. how far apart in time the asynchronously presented audio and visual pair could be perceived as synchronous. The PSS is unique to each individual. Our perception of synchrony (or asynchrony) of audiovisual signals is affected by a variety of factors such as the nature of the stimuli, its complexity, experience, life span, and is especially influenced by time lag (ΔT): time spacing between the tone and flash [129-133]. The behavioral run started with 5s of initial rest followed by the presentation of audio and visual stimuli with a systematically varying asynchrony lag of 66.6, 83.3, 100, 116.6,133.3,150 and 166.6 milliseconds. Previous literature suggested that humans can correctly detect audiovisual asynchrony within these limits [130,133-136]. The time between each pair (the pause, τ) was chosen randomly between 1000- 1160 ms. Participants were seated in a dimly lit room at an approximate distance of 70-80 cm in front of the monitor and responded using a keyboard. On each trial, participants were asked to judge whether the AV stimulus was synchronous or asynchronous. They were asked to indicate their perception by left mouse click if they perceived synchrony or right mouse click for asynchrony. After reporting their perception, participants were asked to click on the middle of the mouse to advance to the next stimulus. Each condition was presented 20 times, totaling 140 trials. After completing the run, we looked at the fraction of the trials that were perceived as synchronous or asynchronous. The time lag (ΔT) was chosen from the sets of time lags in which performance accuracy was 50:50 % or close to it (which we call temporal threshold or simply threshold in this text). The second session also involved acquiring behavioral data and response time outside the fMRI scanner. It consisted of a single run but the time lag (ΔT) were manipulated to a threshold-16.6, threshold and threshold+16.6 ms. The pair of stimuli was presented 60 times: 20 at each ΔT. The time the stimulus was presented and the response time to that stimulus were recorded for further analysis.

Inside the fMRI scanner. The last experimental run was inside the fMRI scanner where fMRI data was acquired and behavioral responses were recorded (Figure 3.1). This fMRI run started with 30 seconds of initial rest followed by 24 multisensory task blocks and 8 blocks of unisensory task. Blocks were presented in a random order and consisted of 8 pairs of stimuli in the multisensory block where both the tone and flash were presented. In the unisensory block, either 8 flashes or 8 beeps were presented. Stimuli within a block were presented with the random pause of 1666 to 1926 ms followed by the cue of 600ms at the end of each block, totaling about 24 seconds for one block. There was about 10 seconds of pause in-between blocks and the run ended with 35 seconds of a final rest period. While running the experimental runs, participants were asked to focus their gaze on the crosshair at the center of the screen.

While recoding our data, two stimulus types were used; a beep-flash pair with a distractor and one without a distractor. No distractor was used in the unisensory block either. Here the distractor was a ball of a radius 0.7 cm moving across the screen, only one time per AV pair, either left to right or right to left while the audio-visual pair stimuli was presented. Participants were asked to disregard the ball and focus on the sensory stimuli. The aim of adding distractor was to make more engaging. The data from these two conditions (with distractor and without distractor) was initially analyzed separately. However we did not find significant behavioral difference in the perception of asynchrony with or without the distractor (mean percentages were 35.43 and 31.66 respectively, probability (p)= 0.49, a paired t-test was performed). Similarly, we did not find significant difference between synchrony response with or without distractor (means 64.56 and 68.33, p= 0.49). Also, no significant difference was found in RT between asynchrony perception with or without the distractor (means were 0.91 s and 1.03 s, p=0.17) and that of synchrony perception too (means were 0.78 s and 0.79, p= 0.87).

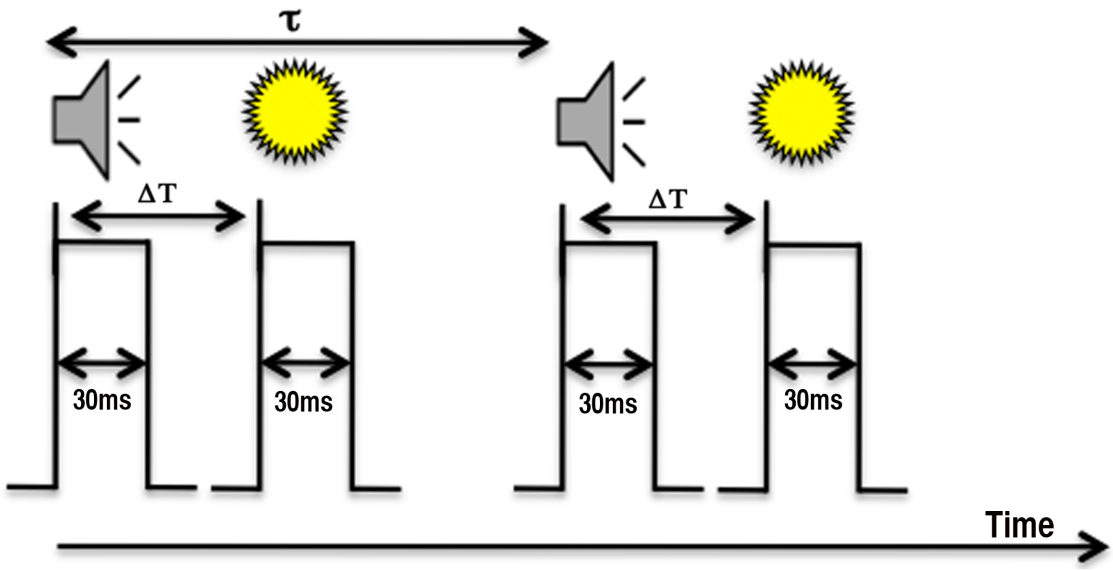

Figure 3.1 Experimental paradigm.
Task paradigm during the functional experiment started with initial 30s of rest followed by task blocks and 35s of rest at the end of the run. There were two block types: multisensory blocks (beep-flash pair were presented for 30 ms, as shown in figure) and unisensory blocks (flash only or beep only were presented, not shown in figure). The time interval between the beep and flash (ΔT) were varied participants to participants. Stimuli within the block were presented with the random pause (τ) of 1666 to 1926 ms followed by the cue of 600ms at the end of each block; totaling about 24 second of one block. Participants were asked to respond after the cue was presented. In unisensory blocks, since a single stimulus was presented, no question was asked about asynchrony and synchrony perception at end of block.

Further, to make sure that there was no significant difference in brain activation, we first analyzed the brain data considering with and without the distractor as a separate regressor in SPM general linear model for both asynchrony and synchrony response trials. We compared mean contrast values extracted form SN nodes using a pairwise t-test. We found no difference in mean contrast values of asynchrony and synchrony perception between with and without the distractor conditions (for lINS: p =0.20 and 0.64, for rINS p=0.95 and 0.07, for dACC p=0.93 and 0.14. Here the first value of p is between asynchrony perception with a distractor and

without a distractor and the second value is that of synchrony perception). So for further analysis we combined the trials of asynchrony perception from with and without the distractor condition and called them as asynchrony on trials and that of synchrony as synchrony trials.

3.2.4 Data Acquisition and Analysis

3.2.4.1 Behavioral data

Response time (RT), the time between onset of the stimulus and button response, for each trial was recorded outside the scanner and behavioral performance was recorded from both inside and outside the scanner. Participants' behavioral performance was analyzed using Matlab. Trial by trial RTs of each participant from outside the scanner were separated and averaged for both asynchrony and synchrony responses. Paired t-tests were used to compare the response times between the asynchrony and synchrony perception conditions. We did not record RTs inside the scanner as the participants were instructed to wait until the question mark (cue) was displayed in the computer screen before indicating their decision by button presses for the given stimuli.

3.2.4.2 Functional magnetic resonance imaging (fMRI) data

The whole-brain MR imaging was done on a 3-Tesla Siemens scanner available at CABI (Georgia State and Georgia Tech Center for Advanced Brain Imaging, Atlanta, Georgia). High-resolution anatomical images were acquired for anatomical references using an MPRAGE sequence (with, TR = 2250 ms, TE = 4.18 ms, Flip angle = 9^0, inversion time = 900 ms, voxel size = $1\times1\times1$ mm^3). The functional run consisted of 449 scans, the measurement of the T2*-weighted BOLD effect, were acquired with a gradient echo-planar imaging protocol; echo time (TE) = 30 ms, repetition time (TR) = 2000 ms, flip angle = 90^0, voxel size = $3\times3\times3$ mm^3, field of view = 204 mm × 204 mm, matrix size = 68×68 and 37 interleaved axial slices each of 3 mm

thickness.

MRI data were analyzed using Statistical Parametric Mapping (SPM8, Wellcome Trust Center, London, http://www.fil.ion.ucl.ac.uk/spm). Functional volumes were slice timing corrected at individual subject level as this step is required to minimize the error in effective connectivity between different brain regions [137]. The further processing steps includes motion correction, co-registration to individual anatomical image, normalization to Montreal Neurological Institute (MNI) template [138] and smoothing of functional scans. Spatial smoothing of the normalized image was done with an 8 mm isotropic Gaussian kernel. A random-effects, model-based, univariate statistical analysis was performed in two level procedures. At the first level, a general linear model (GLM) was specified according to the task sequences and behavioral responses for each participant, rest and six motion parameters were also included in GLM analysis. Here 6 motion parameters were entered as nuisance covariates and were regressed out of the data. After defining the contrast in first level analysis, the contrast images of the particular contrast from all participants were then entered into a second level analysis for a separate one-sample t-test. The resulting summary statistical maps were then thresholded and overlaid on high-resolution structural images in Montreal Neurological Institute (MNI) orientation. For display purposes, the functional images were overlayed on the MNI template available in MRIcro (http://www.mccauslandcenter.sc.edu/CRNL)

3.2.4.3 Effective connectivity analysis: dynamic causal modeling (DCM)

To examine the effective connectivity established by our experimental conditions (i.e. asynchrony and synchrony perception) between our ROIs in SN, we used dynamical causal modeling [139] implemented in SPM8 (DCM10). We identified the ROIs from the group level

results and determined the peak voxels of interest from the contrast [asynchrony (A)+synchrony (S)> beep (b)+flash (f)]. Then we used these coordinates as a reference to find the local maxima from the first level brain map and extracted the eigenvariate by defining a sphere of radius 6 mm for the contrast of interest adjusted for the equivalent F-contrast. The center of each region of interest (ROI) was located on the most significant voxels in the cluster nearest to the peak cluster coordinate obtained from group analysis and activated at the a significance level ($p<0.05$ uncorrected) and lie within twice the width of the Gaussian smoothing kernel used while smoothing the data. Obtained fMRI time-series were then used in the DCM analysis. First, using Bayesian model selection [140], we identified nodes from where the inputs to the SN entered. Second, using Bayesian model averaging (BMA), we computed resultant connection (intrinsic and modulatory) strengths established by our task (i.e., perception asynchrony and synchrony). Finally, we tested for statistical significance of resultant intrinsic connection strengths within SN and determined whether any connections were significantly modulated by task conditions.

For DCM analysis, we kept matrix A, the matrix of intrinsic connections, fully connected between ROIs across all models. For three ROIs, there were six possible intrinsic connections (dACC to RINS, dACC to LINS, RINS to dACC, LINS to dACC, LINS to RINS, and RINS to LINS). The "B" matrix is the matrix of changes (increases or decreases) in effective connectivity between regions for each task condition of interest. As in "A" matrix, there were six possible connections in "B" matrices and each connection could exist in two states (i.e., modulated or not modulated by task type) and, therefore, there are $2^6 = 64$ mathematically possible combinations of "B" matrix. Similarly, The inputs into the network are expressed in matrix "C". It represents the direct influence of the task on specific nodes. For 3 ROIs, there are 7 possible input conditions as: dACC alone, RINS alone, LINS alone, dACC and RINS in combination, dACC

and LINS in combination, LINS and RINS in combination, all nodes. Therefore, we have used 7×64=448 models per participant to thoroughly explore model space. Each of the 64 models of 7 families were compared using the random effects option of the family level Bayesian inference [140] and the winning families were taken to the next level analysis (detail analysis and result : on result section).

3.3 Results

3.3.1 Behavioral performance

Since there is no right or wrong answer, we categorized the behavioral responses based on participants' perception of asynchrony and synchrony. The mean performance ratio outside the scanner was about 34: 66 (standard deviation (std), 19.71) for asynchrony and synchrony perception respectively. However, more time was taken to respond with the asynchrony perception (mean RT =0.96 ms, std 0.30) compared to synchrony (mean RT 0.79 ms, std 0.23). This was statistically significant (student's paired t-test, p=<0.016,t-stat =2.48). Similarly the mean performance ratio inside the scanner was the ratio of 41: 61 (std, 17.58). The plots of behavioral results are shown in Figure 3.2.

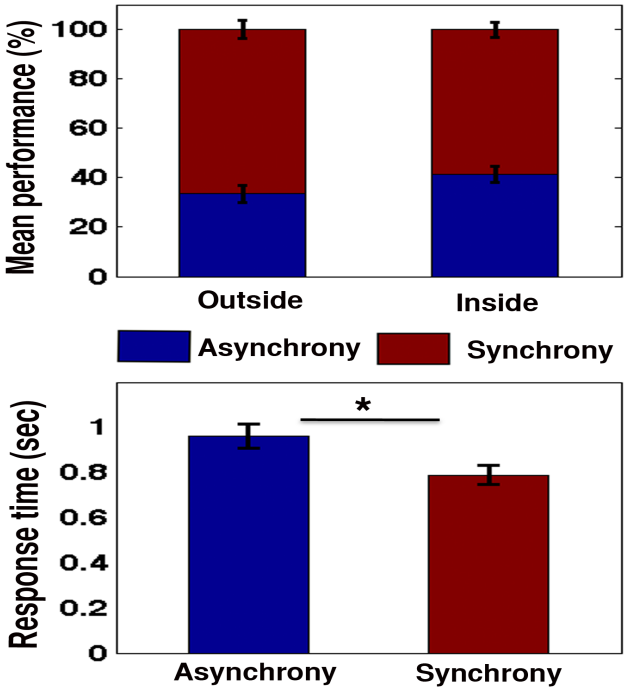

Figure 3.2 Behavior results.
Behavior responses were categorized based on participant's perception of asynchrony and synchrony. The mean performance ratio outside the scanner was about 34: 66 and that of inside the scanner was 41: 59 for asynchrony and synchrony perception respectively (top). The trials by trial response time (RT) were recorded outside the fMRI scanner and mean RT were 0.96 and 0.79 s for asynchrony and synchrony response respectively (bottom). Error bars show standard error of the mean. (* $p < 0.05$).

3.3.2 Brain activation

Both synchrony and asynchrony perception activate the SN network (Table3.1 and Figure. 3.3). The contrast used was asynchrony perception (A)>[auditory (beep only; b) +visual (flash only; f), in other words multisensory > unisensory] and synchrony perception (S)>[auditory (beep only; b) +visual (flash only; f)] respectively. Further, for ROI analysis purpose, we have contrasted [asynchrony perception (A)+ synchrony perception (S)]> [auditory (beep only; b) +visual (flash only; f). From the activation map, we have extracted the contrast values (the beta parameters), by defining a sphere of 6 mm radius centered at the local maxima

peak activity voxel using MarsBaR[66]. The group average of contrast values was plotted for each node in SN separately for asynchrony and synchrony conditions (Figure 3.3B). We found significantly (paired t-tests) higher brain activity in asynchrony perception compared to synchrony perception conditions in each node of SN.

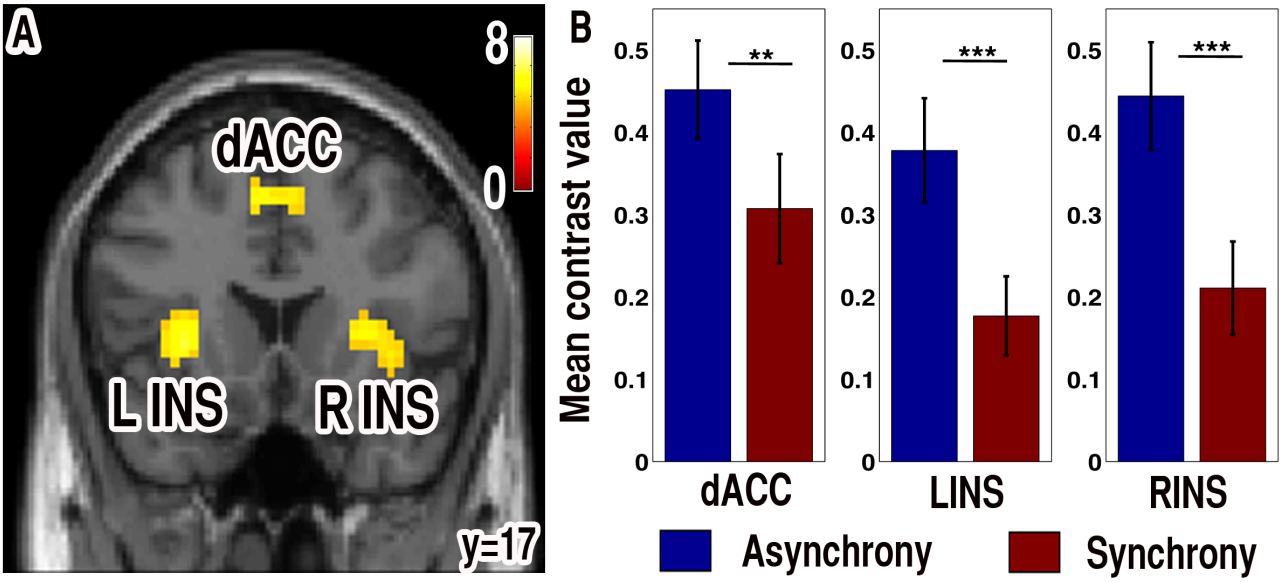

Figure 3.3 SN activation.
(A) Brain activations shown were associated with contrast: asynchrony (A) and synchrony (S) (i.e. multisensory stimuli) > beep (b)+ flash (f) (i.e. unisensory stimuli) . Final statistical images were thresholded using family-wise error (FWE) correction of multiple comparisons at p <0.05. (B) Plots of mean contrast value associated with asynchrony and synchrony perception in SN nodes. Error bars show standard error of the mean. ** = p<0.01, and *** = p<0.005)

Table 3.1 Brain activations for asynchrony perception (A) and synchrony perception (S) contrasted with audio (beep, b) and visual (flash, f).

Contrast	Brain area	MNI coordinates (x, y, z)	Cluster size	Z (t-stat)
A>b+f**	Dorsal anterior cingulate (dACC)	-6 11 52	203	6.93 (10.71)
	dlPFC(BA9)	-60 8 31	79	9.13 (6.36)
	Insula (R INS)	33 20 4	169	6.24 (8.82)
	Insula (L INS)	-30 20 4	103	5.85 (7.93)
	Visual area (BA 18)	27 -97 -2	62	5.82 (7.84)
	Inferior perital lobe (IPL)	-30 -49 46	71	5.63 (7.45)
	Thalamus	3 -1 1	19	5.56 (7.27)
	Medial Globul Pallidus	-12 2 1	33	5.41 (6.99)
	Caudate body	15 8 7	49	5.39 (6.96)
	dlPFC (BA9)	45 2 28	57	5.22 (6.63)
	Visual Area (BA17)	-30 -94 -8	19	5 (6.22)
S>b+f *	Visual area (BA 18)	27 -97 -8	90	5.97 (8.19)
	dACC	-9 11 49	96	5.64 (7.46)
	Thalamus	3 -4 1	88	5.55(7.29)
	Visual Area (BA18)	-27 -94 -5	62	5.45 (7.07)
	dlPFC	-60 8 25	16	4.97 (6.17)
	Insula (L INS)	-30 20 7	56	4.61 (5.55)
	Insula (R INS)	33 23 7	41	4.44 (5.28)
	Inferior perital lobe (IPL)	-33 -46 43	27	4.38 (5.18)
A+S>b+f**	dACC	-6 11 52	122	6.61(9.78)
	Visual area (BA 18)	27 -97 -5	71	6.24 (8.84)
	dlPFC	-60 8 28	47	6.07 (8.42)
	Thalamus	3 – 1 1	101	6.07 (8.41)
	Insula (L INS)	-30 20 4	84	5.78 (7.76)
	Insula (R INS)	33 23 4	117	5.75 (7.69)
	BA18/lingual gyrus	-27 -94 -5	37	5.31 (6.80)
	IPL	-30 -49 46	42	5.24 (6.67)

** Family-wise error corrected (FWC) <0.05, *AlphaSim corrected p<0.05

3.3.3 Dynamical causal modeling analysis (DCM)

To identify where the inputs to the SN entered, family level inference was used. This procedure removed the uncertainty about aspects of the model structure other than the

characteristic of interest. For example: what are the inputs to the system? [140]. Out of seven family models we have compared, the most evidence (xp, the exceedance probability) was for right insula input (83.12%). Similarly the evidence for dACC and left insula input was 8.50% and 7.90% respectively. The evidences for remaining families were less than 0.33% (Figure 3.4A). We focus our further DCM analysis on the first three winning models as the evidence combining three families resulted 99.51%.

The random effect Bayesian model averaging procedure (BMA.rfx) was used to compute resultant pattern of connection strengths (intrinsic and modulatory) established by the perception of asynchrony and synchrony of AV pairs. The intrinsic connections between nodes during asynchrony and synchrony perception were found significant (t-test, $p<0.05$) from (i) R INS to L INS and dACC (ii) L INS to R INS and dACC (Figure 3.4B,blue arrows). No significant connections were observed from dACC to R INS and L INS. Next, we investigated whether the connections were modulated by asynchrony and synchrony conditions (the matrix "B"). For the asynchrony condition, the connection from L INS to R INS was significantly increased (Figure 3.4B,red arrow). No other connections were found to be modulated by either asynchrony or synchrony perception. The parameter estimates of the driving stimuli to dACC, left and right insula were found to be 0.027, 0.020 and 0.030 respectively.

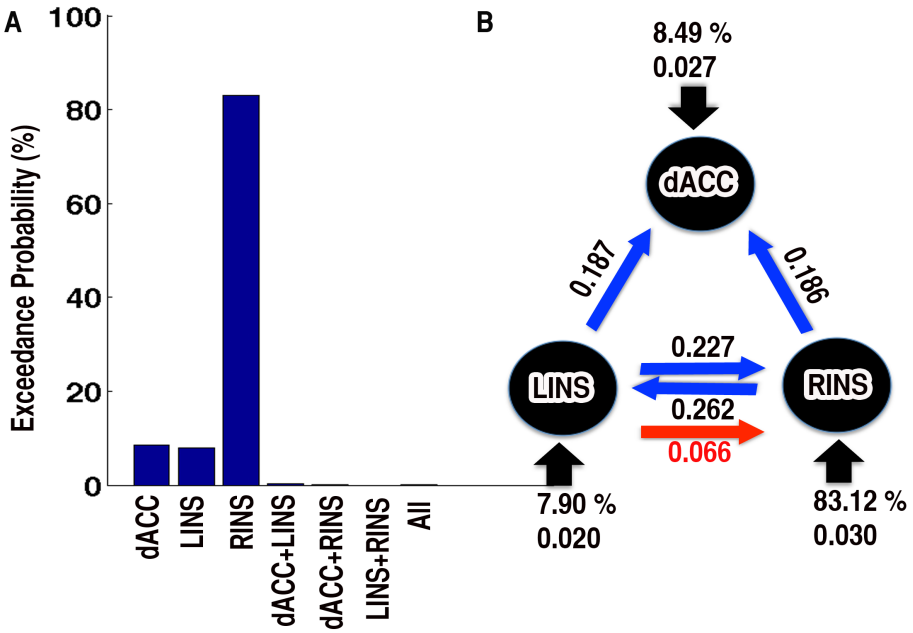

Figure 3.4 Exceedance probability and connections between nodes of SN.
(A) The bars represent the exceedance probability of constructed seven families based on where the input was supplied to the SN. (B) Schematic representations of significant connections and parameter estimates of driving stimuli obtained from Bayesian model averaging from the first three winning families. The blue arrows: significant intrinsic connectivity between nodes and red arrow increased effective connectivity from LINS to R INS for asynchrony perception condition. The number next to the arrows represent respective connection strength. The xp (the exceedance probability) and the parameter estimates of driving stimuli of the node are shown with large arrow.

3.4 Discussion

The INSs and the dACC form an independent brain network, the salience network (SN) [36]. These brain regions are often co-activated, making it difficult to isolate the functional role of individual nodes [141]. In this study, we attempted to understand the complex, and as yet only partially characterized patterns of functional connectivity between nodes in the human SN by using the multisensory perception task coupled with dynamical causal modeling (DCM). Our DCM analysis showed that both R INS and L INS were connected intrinsically to each other and also with dACC. Input to the SN mostly came through R INS. These results suggest a central

role of INSs and dACC in the perception of sensory events and selection of appropriate behavioral responses. These findings further extend previously reported findings that the INSs and dACC serve as part of the decision-making network that integrates information important to choose one response over another [22,23,25-27,120,126].

A large number of studies have found that the insula is a key structure in perceptual decision-making [22,111-113,116]. INSs have been shown to have widespread efferent and afferent projections to and from both the frontal and parietal cortices [124,142,143]. This connectivity places the INSs perfectly to perform their putative role on decision-making, for example INSs are involved in integration [114,115] and comparison [111,144] of sensory information. The significantly higher brain activity (Figure 3.3B) in INSs during asynchrony perception might reflect the greater task difficulty in audio-visual integration [116,145] and discrimination [146].

The dACC has been implicated as part of the task-set system that initiates and selects action [21]. Lesions in this part of the brain can lead to difficulties in initiating complex voluntary movements and actions [25,119,120]. However, in goal directed actions, knowledge about which task to pursue is important before we initiate or select any action. This is done by accumulating evidence to support one action over another action [147,148]. The significant intrinsic connectivity form INSs to dACC in our task condition supports the previous findings that the dACC gets immediate access to information about external task cues from insular cortex, cortical areas associated with high-level perception [149,150]. In our task condition, dACC might be involved in accessing moment-to-moment perceptual information supporting one versus another response in order to guide behavior. The higher brain response in dACC during asynchrony perception compared to synchrony perception might be due to the increased task

demand of assessing information required for response selection processing, such as conflicting information which may make such selection difficult [120,151]. This is in line with previous findings that dACC facilitates response selection under conditions of conflicting response alternatives or task sets [123,152]. The role of dACC in the decision-making process includes action initiation [25] and the selection of specific actions [120], dACC's role is also supported by the findings in a much wider range of decision-making tasks [22,23,26,126].

INSs and dACC share a direct white matter connection [124]. There is now a wealth of evidence that INSs and dACC have a close functional relationship in wide range of tasks [20,24,32,36,111,112,125]. SN plays a role in the coordination of behavioral responses [121]. Our findings provide evidence that efficient behavior evolves from the causal interaction of nodes within the SN. The higher evidence that input in SN is mostly from INSs suggests their role in the integration of stimulus saliency [27,114,115]. This is supported by INSs widespread efferent and afferent projections to and from both the frontal and parietal cortices [124,142,143]. Activity in dACC was triggered by INSs, which has led to the conclusion that INSs provide cortical signals used for appropriate response selection. This is in line with previous findings that suggest the insula acts as a cortical "out flow hub" to influence activity of other brain regions [24,32,153].

The input to the right insula was much higher than to the left insula (Figure 3.4B), which suggests a dominant role of the right insula in the SN function. This difference of the left and the right in the insular function has not been understood well, possibly because they are usually co-activated [117,154-156], as in our current study. Here, by the use of DCM, we were able to point out that there might be different functional roles of the left and right insulae in the integration of perceptual saliency. Based on these results and experimental evidence obtained

from other similar studies [24,32,157], we propose that the right insula is, in general, critical for the integration of external stimuli in a perceptual decision process, in which the interactions between the left and the right insulae are essential. Highly engaging tasks such as the asynchrony perception task that we conducted often lead to modulation of effective connectivity from the left to the right. These results are consistent with the earlier proposal that the right insula aids in the coordination and evaluation of task performance across behavioral tasks with varying perceptual and response demands [157].

Broadly, our results support that SN is a set mechanism required during the performance of cognitively demanding goal-directed tasks [20,21,151] and coordination of behavioral responses [121]. One potential limitation of our study is that we constrained our study within the SN as, in many situations, the activity within SN appears related to goal directed decision-making, especially in engaging tasks [20,21,121,151]. However, these were not the only higher order cortical brain regions activated by our experimental task. The other brain regions activated included the dorsolateral prefrontal cortex (dlPFC) and inferior parietal lobe (IPL). The dlPFC has been reported in various decision-making tasks [31,158-161], and is also considered a part of the cognitive system [84,162,163]. Another brain region, IPL, has also been reported in various decision-making tasks [164-168]. The thalamus is known to be involved in perceptual task [169]. In our study also, the thalamus was strongly activated both in synchrony and asynchrony conditions. Thalamus did not show significant difference in modulation of activity levels by the perception of synchrony and asynchrony (paired t-test, $p=0.63$). However, resolving effective connectivity patterns between the salient network and the thalamus would definitely add to our current understanding of salience information processing in the brain. But, we leave this computation for future research since the DCM analysis to resolve this connectivity pattern will

be computationally expensive due to a large number of models that need to be solved for a connectivity of four nodes with inputs and modulations included per participant.

Finally, we provide evidence about how the nodes in the SN played their role in the decision-making process and implementation of goal-directed action. The INSs were found to a play an important role in integration of sensory information. INSs also supply necessary information for the dACC to use for the selection of the appropriate response. The present results support the hypothesis that dACC and INS are part of the task-set system involved in the decision-making process, and that this mechanism is required during the performance of cognitively demanding goal-directed tasks.

4 PERCEPTUAL DECISION-MAKING DIFFICULTY MODULATES FEEDFORWARD EFFECTIVE CONNECTIVIRTY TO DORSOLATERAL PREFRONTAL CORTEX.

4.1 Introduction

Humans are efficient in perceiving and discriminating the visual objects. How does the brain receive, relay, and integrate relevant sensory information to make such perception and discrimination known as perceptual decision? Specifically, what are the brain regions involved and how do these regions coordinate activity in perceptual decision-making processes? Previous studies showed that the brain areas on the ventral visual pathway process object category-specific visual information [35,170-172]. However, visual information processing in these early visual areas was found insufficient in discrimination of visual objects [173-175]. In spite of the abundant research in the field [19,33,170,172,176-178], we do not exactly know where and how visual information is processed in the brain to arrive at a difficult perceptual decision. In this

study, we used face-house categorization tasks with three levels of noise in face-house images in functional magnetic resonance imaging (fMRI) experiments to answer these questions.

The encoding of relevant sensory information is one of the main steps of the brain processes in the cognitive chain leading to perceptual decisions. Experiments on both humans and non-human primates have demonstrated that the first stage of perceptual decision-making involves lower order regions receiving and representing sensory information [37,113,179-182]. For example, perception of faces showed stronger response in the fusiform face area (FFA) [35] and that of house in the parahippocampal place area (PPA) [39,170,183,184]. However, relatively recent studies in the field have shown that the representation of visual information in these areas, also called core system, is not sufficient [173,174,185,186], and further processing of visual information in the higher order cortical area, also called the extended system, is crucial to discriminate visual objects [19,173,176].

In a previous study, the core system was found to be functionally organized in a hierarchical, feed-forward architecture, in which the core exerted a strong causal influence on the extended system in frontal cortex [176]. The frontal cortex activity, especially in the dlPFC, was also reported in semantic analysis [187], disambiguation [159], and temporal processing [188]. The dlPFC was also found to be involved in social decision-making [2,47,161] and cognitive control [83]. The dlPFC has been understood to accumulate relayed sensory information to form a decision [189]. However, how these regions in core and extended system coordinate activity in relaying and integrating competing sensory information to arrive at perceptual decisions is largely remained unknown.

Here, we aimed to map out the neural mechanisms for perceptual decision-making processes by examining categorization-task specific brain activations, brain connectivity, and

their modulations by decision-making task difficulty. We included three-noise levels in our stimuli, predicting an increase in connectivity within category-specific brain areas in ventral temporal region (the FFA and the PPA) and feedforward connectivity between these regions and the extended system (the dlPFC) by face-house categorization difficulty. The rationale for this prediction is based on the notion that as noise in face-house stimuli increases, the neural representation of category specific information in FFA and PPA decreases [38]. As the result of the decrease in category specific information in these regions with noise, the brain has to work harder in gathering and evaluating of sensory information and hence predicted increased activity in decision-making [159,160,187,189].

4.2 Materials and Methods

4.2.1 Participants

Thirty-three human participants (17 females; mean age 27.54 ± 4.67 years) participated in this study. All participants had normal or corrected to normal vision and reported normal neurological history. Participants provided written signed informed consent forms and were compensated for their participation in the experiments. Institutional Review Board (IRB) for Joint Georgia State University and Georgia Institute of Technology Center for Advanced Brain Imaging, Atlanta, Georgia, USA approved this study.

4.2.2 Stimuli

We used a total of 14 images of faces and 14 images of houses as stimuli. All the presented pictures were downloaded from F.A.C.E. Training–an interactive training by Paul Ekman (https://www.paulekman.com/product/pictures-of-facial-affect-pofa/). All the images were equalized for luminance and contrast by converting them to gray scale and were cropped to

make equal size. Furthermore, both face- and house- images were degraded by manipulating images and adding noise [190]. Image pixel phase randomization and addition of Gaussian noise enabled us to make visual image stimuli noisy. Stimuli consisted of three different noise levels: 0 %, 40%, and 55%, for both sets of images. The stimulus software Presentation (http://www.neurobs.com) was used to display stimuli and to control task trial sequences.

4.2.3 Task and behavioral paradigms

The experimental task was divided into two separate sessions: the first session involved acquiring behavioral data outside the MRI scanner and the second session was inside the scanner, where we acquired both fMRI and behavioral data. In both cases, participants were asked to decide whether the presented gray scale images were faces or houses. They indicated their decisions by keyboard or button presses on a response box. Prior to the experimental tasks, participants were briefly explained about the study and the task. Some sample stimuli were shown and the participants were asked to make decisions about the presented stimuli, allowing them to be familiar with the task.

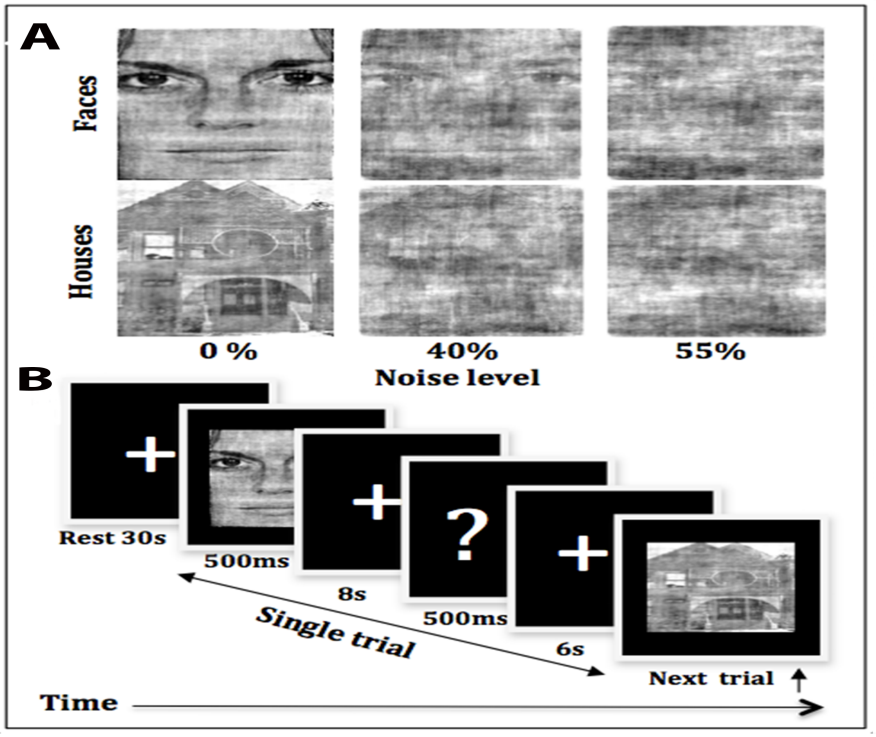

Figure 4.1 Experimental paradigm.

(A) Sample images at three noise levels for sets of both face and house stimuli. (B) Task paradigm during a functional run, starting from the initial 30 s rest followed by a task trial that included 500 ms- stimulus presentation, 8 s of decision time, and 500 ms-display of a question mark, requiring participants to indicate their decision within the next 6 s.

4.2.3.1 Outside the fMRI scanner

This behavioral study consisted of a single run. There were three noise conditions and each condition was repeated 60 times (30 times each for faces and houses) in a random order, generating 180 trials in total. Participants were asked to indicate their decisions as quickly and as accurately as possible by the right and left mouse clicks (right for house stimuli and left for face stimuli). They were instructed to press the space bar in the computer keyboard to proceed to the next trial. The type of stimuli, the stimulus presented times, and the response times to that stimuli were all recorded.

4.2.3.2 Inside the fMRI scanner

Participants performed face-house categorization tasks in three functional runs, each run was 614 s long. The number of trials for each noise condition was 36 (18 faces and 18 houses), and the total trials were 108 for all 3 conditions in each run. Stimuli were presented in a random order as in an event-related design within each run. There were rest periods of 30 s at the beginning and of 35 s at the end of each run. Participants were instructed to focus on the central crossbar on the screen during experimental run. They were asked to perceive the presented stimuli, to wait for the display of a question mark on the screen and then to indicate their choice by pressing a response key on a button-box by using either the index or the middle finger of their right hand. Each picture was presented for 500 ms, followed by an 8 seconds-long display of the fixation cross, then a briefly presented question mark for 500 ms at the end of this 8 seconds' interval. The next 6 s time period was allowed for participants to report their decisions by responding on a button box. Trials in which participants were failed to respond were discarded from the final analysis. Figure 4.1B shows a schematic representation of the behavioral paradigm used in the experiment.

4.2.4 Data Acquisition and Analysis

4.2.4.1 Behavioral data

A participant's response time (RT), the time between the onset of a stimulus and the button press in each trial was recorded for the tasks performed outside the scanner. Participants were required to do button presses only to indicate their decisions inside the scanner. Participants' behavioral performance, both outside and inside the scanner, was analyzed by using Matlab. Trial by trial RTs of each participant from outside-scanner button presses were separated

and averaged across noise conditions. No RT calculation was done for the recorded behavioral data inside the scanner as participants were instructed to wait until the question mark was displayed to indicate their decisions. T-tests were used to assess the significance levels of performance accuracy and response time across noise levels in face-house stimuli.

4.2.4.2 Functional magnetic resonance imaging (fMRI) data

The whole-brain MR imaging was done on a 3-Tesla Siemens scanner available at Georgia State University and Georgia Institute of Technology Center for Advanced Brain Imaging (CABI), Atlanta, Georgia. High-resolution anatomical images were acquired for anatomical references using an MPRAGE sequence (with TR = 2250 ms, TE = 4.18 ms, Flip angle = 90^0, inversion time = 900 ms, voxel size = $1\times1\times1$ mm^3). Three functional runs each of 307 scans with the measurement of the T2*-weighted BOLD effect, were acquired with a gradient echo-planar imaging protocol and these parameters: echo time (TE) = 30 ms, repetition time (TR) = 2000 ms, flip angle = 90^0, voxel size = $3\times3\times3$ mm^3, field of view = 204 mm × 204 mm, matrix size = 68×68, and 37 axial slices each of 3 mm thickness.

MRI data were analyzed using Statistical Parametric Mapping (SPM8, Wellcome Trust Center, London, http://www.fil.ion.ucl.ac.uk/spm) which included slice timing correction, motion correction, co-registration to individual anatomical image, and normalization to Montreal Neurological Institute (MNI) template [138]. Spatial smoothing of the normalized image was done with an 8 mm isotropic Gaussian kernel. A random-effects model-based univariate statistical analysis was performed in two level procedures. At the first level, a separate general linear model (GLM) was specified according to the task sequences and behavioral responses for each participant. Only correct trials for each of the three noise-levels (0%, 40% and 55%), rest and six motion parameters were included in GLM analysis. Here, 6 motion parameters were

entered as nuisance covariates and were regressed out of the data. Individual contrast images of all participants from the first level analysis were then entered into a second level analysis for a separate one-sample t-test. The resulting summary statistical maps were then thresholded and overlaid on high-resolution structural images in Montreal Neurological Institute (MNI) orientation. For display purposes, the functional images were overlayed on the MNI template available in MRIcro (http://www.mccauslandcenter.sc.edu/CRNL).

4.2.4.3 Brain Activity and Effective Connectivity Analysis

We examined the brain activity of hypothesized regions of interest (ROIs) in our experimental condition (i.e. face-house discrimination task at different noise-levels). We defined the ROIs from the group level activation results. To localize FFA activation in-group level, we used face>house contrast. Similarly to localize PPA, we contrasted house with face (house>face). The peak-activity location of the dlPFC was chosen using face + house > rest contrast. The ROIs analysis were performed using a spherical region of 6 mm radius centered at the maxima peak activity voxel of group level result using MarsBaR[66]. The beta parameters (also called contrast values) were extracted for each experimental condition that was defined in design matrix for each subject. The beta parameters of condition of interest were then averaged over the subjects. Finally, paired t-tests were used to determine whether there was a statistically significant difference in contrast values between the conditions of interests.

The effective connectivity established by our experimental conditions between ROIs were examined using dynamical causal modeling [191-193] implemented in SPM8 (DCM10). For this purpose, we used group level peak activity coordinates as a reference to find the local maxima from the first level brain map. Then we extracted the eigenvariate by defining a sphere of radius 6 mm for the contrast of interest adjusted for the equivalent F-contrast. While

extracting eigenvariate, the center of each ROI was positioned on the most significant voxel in the cluster nearest to the peak cluster coordinate obtained from group analysis and activated at the a significant level ($p<0.01$ uncorrected), and lie within twice the width of the Gaussian smoothing kernel used while smoothing the data. The details of modal specification and comparison procedure were included below.

4.3 Results

4.3.1 Behavioral response.

The mean performance (i.e. the group level accuracy) for images with 0% noise-level was very high. The accuracy rate for 0% noise was 99.26 for outside scanner and that of inside the scanner was 97.89%. The performance levels were found decreased for 40 % noise-level and the rates were 89.48% and 87.01% for outside and inside the scanner respectively. The rates were further decreased to 68.52% and 65.07% for outside and inside the scanner respectively when the noise level increased to 55%. A paired t-test was performed to see the significant effect of task difficulty (or, noise-level) on behavioral accuracy. The behavioral accuracies were found decreased significantly (all $p < 0.001$) with noise level (Figure 4.2). On the other hand, RTs were found significantly increased with noise level (all $p< 0.01$). The mean response time for clear images (0% noise) was 0.79 s and that for 40% noisy-images was 0.94 s. The response time further increased to 1.13 s for 55% noise level (Figure 4.2).

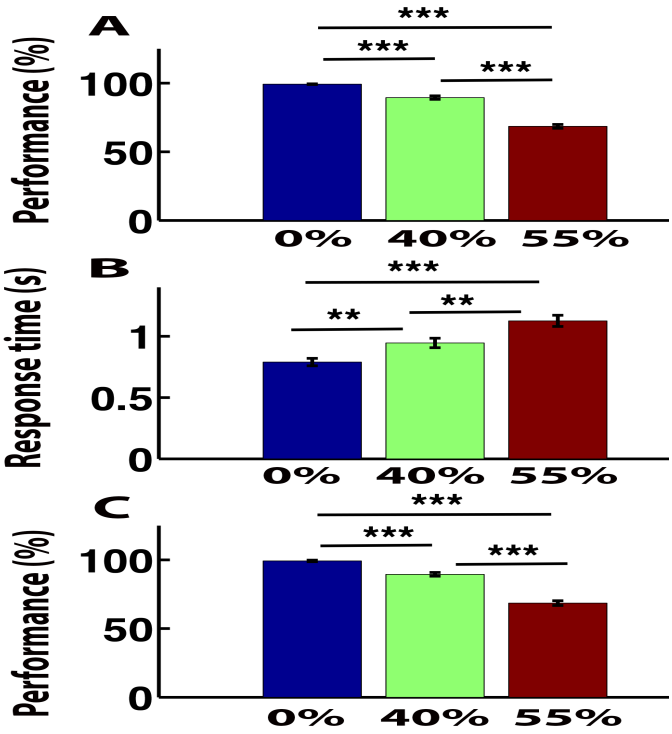

Figure 4.2 Behavior response.
The bar plots of (A) mean performance (%) outside the scanner, (B) response time outside the fMRI scanner and, (C) mean performance (%) inside the fMRI scanner for three noise-levels. (**p<0.01 and ***p<0.001).

4.3.2 Brain Activations

With the face-house decision versus rest contrast, we observed significant brain activations in the occipital, lateral occipital cortex (LOC), FFA and PPA in the ventral temporal cortex (VT), inferior parietal lobe (IPL), dorsolateral prefrontal cortex (dlPFC), insular cortex (INS), and pre-supplementary motor cortex in middle frontal cortex (Pre-SMA) (Figure 4.3 (A, B)). To localize the category specific brain regions in VT, we further contrasted face versus house and house versus face conditions (Table 4.1). The face versus house contrast showed a stronger response in the FFA (Figure 4.3D). Similarly, the house versus face contrast activated PPA more (Figure 4.3C). The ROI analysis showed higher BOLD responses for face in FFA and that of house in PPA (Figure 4.4A). The average beta linearly increased with the difficulty of

task in the dlPFC (Figure 4.4B)

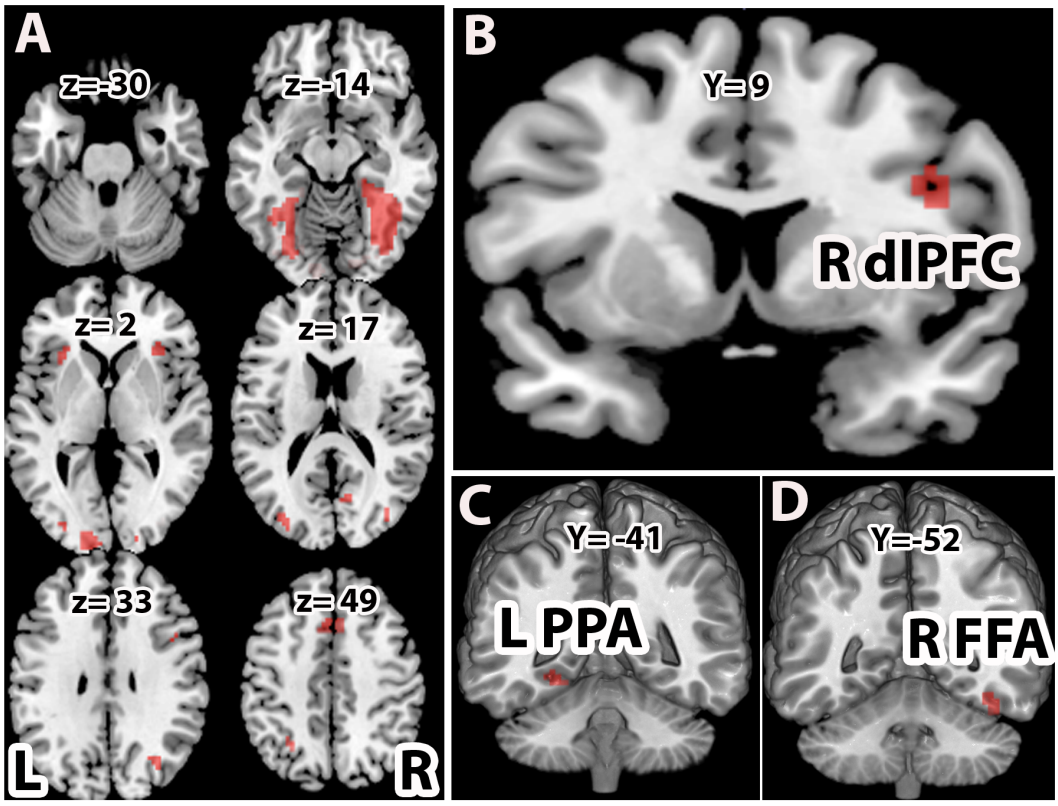

Figure 4.3 Brain activations.

Activations associated with (A) face and house stimuli> rest($p<0.001$)., (B) right dlPFC for face and house > rest ($p<0.001$). (C) Left PPA for house > face ($p<0.05$), and (D) right FFA for face>house ($p<0.05$). All activations are familywise error corrected (FWC).

Table 4.1 Brain activations of face-and-house perception.

Contrast	Brain area	MNI coordinates (x, y, z)	Cluster size	Z -score
Face>House*	Fusiform face area (FFA)	42, -49, -17 (R)	31	4.33
House>Face*	Parahippocampal place area (PPA)	-27, -46, -8 (L)	27	5.64
All pictures>Rest***	Inferior parietal lobe (IPL)	-27, -58, 46 (L)	12	5.69
	Pre-supplementary motor area (Pre-SAM)	-3, 14, 49 (L)	49	6.64
	Dorsolateral prefrontal cortex (dlPFC)	42, 8, 25 (R)	32	6.35
	Insula	33, 26, 7 (R)	38	6.29
		-30, 26, 1 (L)	24	6.15
	Venteral temporal cortex (VT)	30, -46, -14 (R)	489	7.62
		-27, -55, -11 (L)	383	9.91
	Occipital cortex	15, -85, -8 (R)	489	9.42
		-12, -100, -4 (L)	383	7.13
	Posterior cingulate (PCC)	12, -70,13 (R)	41	6.06

R=Right, L=left. Family-wise error corrected (FWC) at *p< <0.05 and ***p< <0.001

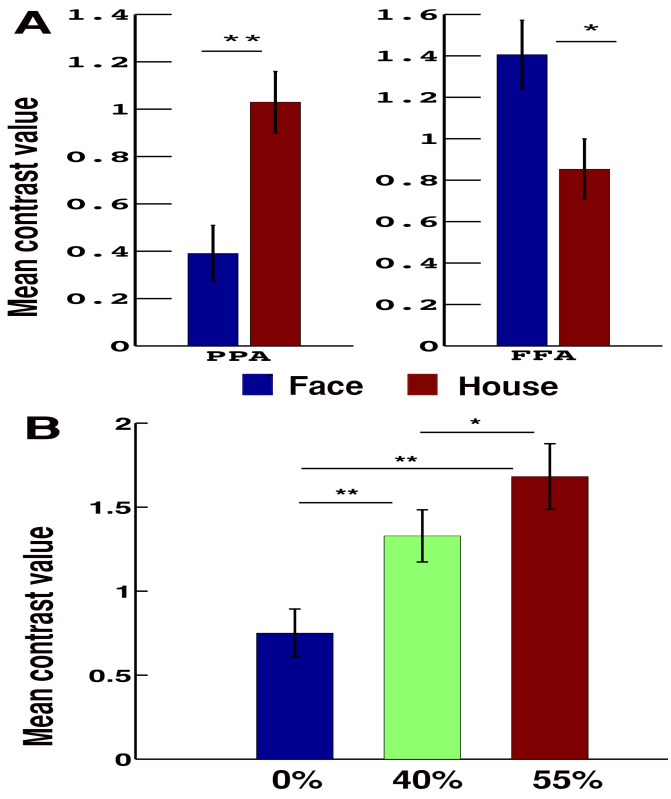

Figure 4.4 Bar plots of mean contrast values.

(A) Contrast values for face and house stimulus conditions in parahippocampal place area (PPA) and fusiform face area (FFA). (B) Contrast values according to the noise-level in dorsolateral prefrontal cortex (dlPFC) (*p<0.05 and ** p<0.01).

4.3.3 Dynamic causal modeling (DCM) results

Based on the hypothesized roles of these regions: dlPFC, FFA and PPA and the network as a whole in face-house decision tasks, we considered various DCM models as shown in Figure 4.5. We defined 8 models for the network consisting of the dlPFC (region 1), FFA (region 2) and PPA (region 3) allowing sensory inputs and modulations. The 'minimal' model (model 1) was systematically modified by adding connections and inputs to build other models (model 2 to model 8). In these models, both face and house trials were used as input on both FFA and PPA. Furthermore, we extended our model space to 16 aiming to remove the uncertainty about aspects of the model structure other than the characteristic of interest. In these additional 8 models face trials were used as input to FFA and house trials to PPA. The random effects Bayesian model selection procedure was then used to select the optimal model at the group level [193].

Out of 16 plausible models, the most evidence favored the model 8 compared to other models (Figure 4.6A). The exceedance probability of the winning model was found 0.54. This model consisted of bidirectional connection between all three regions. Since the test of our hypothesis was based on encoded connectivity parameter that tell us the details about the strength of intrinsic as well as the modulatory effects on connection between ROIs at three noise conditions, we inclined towards Bayesian parameter averaging procedure (BPA) over the winning model. During perception, the intrinsic forward connections from category responsive regions, the FFA and the PPA to dlPFC were 1.72 (posterior probability (p), 1.0) and 1.52 (p=0.99) respectively while the backward connections from dlPFC to FFA and PAA were 0.45 (p=0.82) and 0.29 (p=0.72) respectively (Figure 4.6 B).

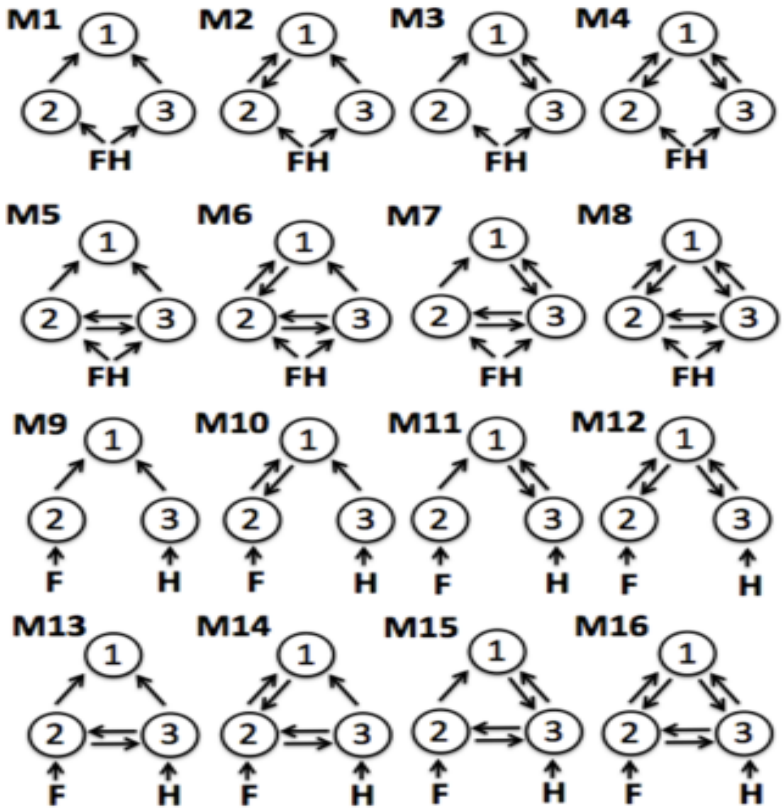

Figure 4.5 DCM model specifications.
Model number 1 is a basic model that included the minimal number of connections between dlPFC (1) with FFA (2) and PPA (3). The endogenous connectivity of this 'minimal' model was then modified by systematically adding connections (from model 2 to 4). Models 5 to 8 were constructed model from 1 to 4 by adding bidirectional connections between FFA and PPA. In these models (1 to 8), all face- house images were the inputs to both FFA and PPA. We further used face image input to FFA and house input to PPA and expanded our model space to 16.

Our analysis further revealed that the bidirectional interactions between FFA and PPA. The coupling strength from FFA to PPA is 1.44 (p=0.99) and that from PPA to FFA is 1.06 (p=0.99). Second, we examined the modulatory effect, the increase in connectivity between regions (Friston et al., 2003) due to the task context on intrinsic connections. The connectivity from FFA to dlPFC was enhanced by 24.88 %, 21.50 % and 9.58 % for image noise levels of 55%, 40 % and 0% respectively and that from PPA to dlPFC was 22.0 %, 18.51 %, and 11.39 %

(Table 4.2). Moreover, we found the significant correlation between feedforward connectivity from FFA and PPA to dlPFC for all noise levels with that of contrast values in dlPFC (Figure 4.7).

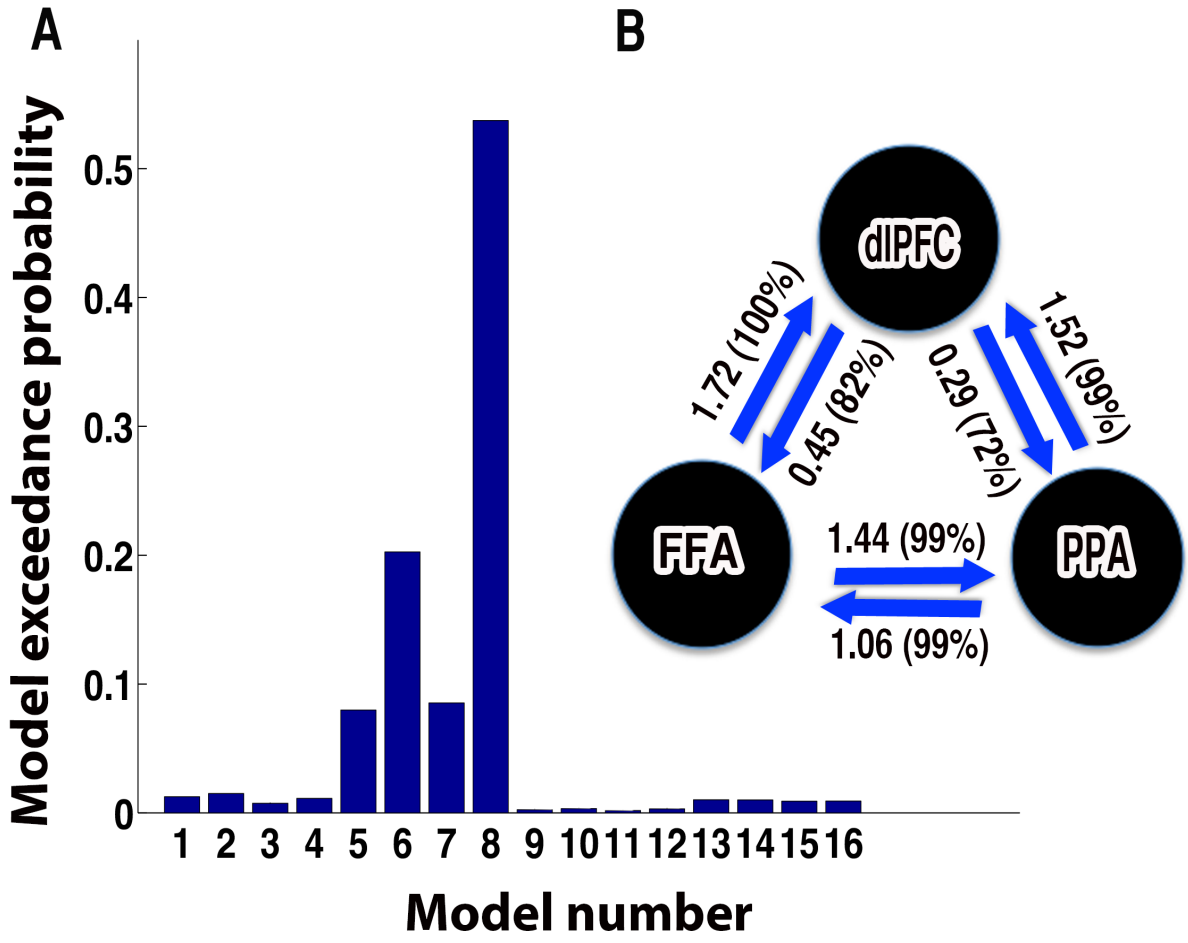

Figure 4.6 Bar plots of exceedance probability for 16 models.

(B) Diagrammatic representation of connectivity patterns between ROIs. Parameters were averaged (Bayesian Parameter Averaging, BPA) across all participants. The numbers next to the connectivity-strength inside the bracket represent the posterior probability (p) of that connection.

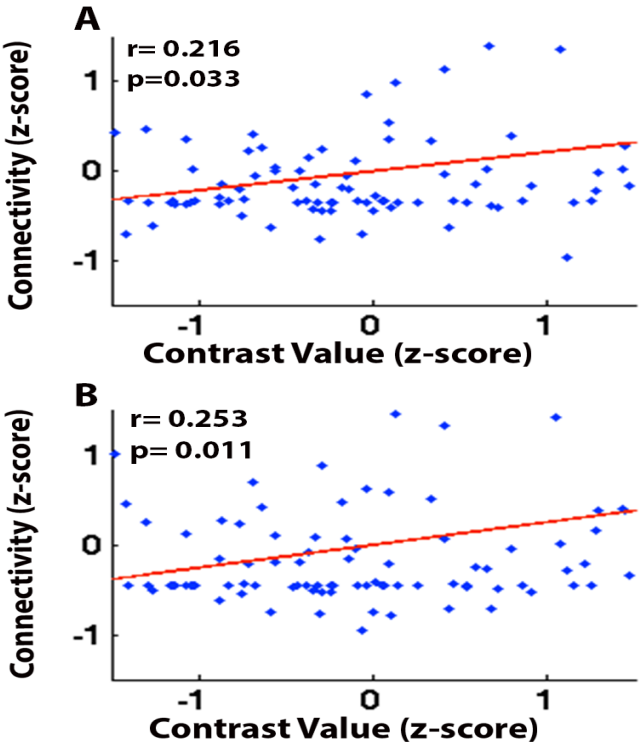

Figure 4.7 Linear fits of connectivity versus contrast value. The plots of connectivity strength from FFA to dlPFC (A) and from PPA to dlPFC (B) with contrast value in dlPFC (in all three-noise level).

Table 4.2 The percent (%) change in effective connectivity compared with intrinsic connectivity.

From	To	Noise level	(%) Change
FFA	dlPFC	0 %	9.58
		40 %	21.50
		55 %	24.88
	PPA	0 %	5.18
		40 %	12.63
		55%	14.20
PPA	dlPFC	0 %	11.39
		40 %	18.51
		55 %	22.00
	FFA	0 %	10.28
		40 %	13.63
		55%	25.09
dlPFC	FFA	0 %	0.66
		40 %	1.96
		55 %	1.76
	PPA	0 %	0.80
		40 %	1.90
		55%	2.67

4.4 Discussion

Here, we investigated the brain activity, effective connectivity and modulations of activity and connectivity by task difficulty during perceptual decision-making in the visual domain. Consistent with previous findings [33,170-172,177,194], we have identified two category-responsive regions FFA and PPA in ventral temporal (VT) area of the brain and the prefrontal region (dlPFC), the decision-making hub. We focused our study on these three regions and applied the Bayesian model selection technique to dynamic causal models in order to select the best neural architecture that account for neural processes of the perception of faces and houses. The group level averages of connectivity parameters between FFA and PPA were found significant and were correlated with the task difficulty. Importantly, we observed dominant feedforward connectivity from these regions to the dlPFC, which also increased with noise level.

We have measured the decision-making difficulty behaviorally both in terms of performance accuracy and response time. The result showed that noise added to face or house images made perceptual categorization decisions difficult. We investigated large-scale brain network and its architecture involved in the task. Out of 16 plausible intrinsic models between FFA, PPA and dlPFC, the model 8 consisting of bidirectional connections between all the ROIs came out to be the optimal model. The observed dominant feedforward intrinsic connectivity, also known as average connectivity established by task from these brain regions to more anterior regions of the brain, the dlPFC in particular, is consistent with the proposal that ventral visual system is the pathway for relaying and processing sensory information of visual objects [35,39,170,183,184].These results are also consistent with the function of the visual system that it may not be involved in a higher order perceptual analysis [112] but may provide a causal input to the extended system [176,195,196] and the relayed sensory information is further processed

by downstream processing areas to produce visual perception [174,175].

The intrinsic connectivity from FFA and PPA to dlPFC was found to be modulated by task difficulty. Further, the modulation of feedforward connectivity to dlPFC and brain activity in dlPFC by task difficulty is consistent with the notion that the brain required more effort to accumulate sensory information together from ambiguous sensory information before a decision about stimulus category can be formed [31,159,160,187]. Here, the function of the dlPCF also fits with its role in disambiguation [159] and in decision-making [83,84,163]. The greater response to the noisy but recognized stimuli [189] in dlPFC further supports its role in evaluation of sensory information [160].

The strengths of intrinsic connectivity from dlPFC to FFA and PAA were 0.45 ($p=0.82$) and 0.29 ($p=0.72$) respectively. The more evidence in favor of model 8 compared with model 5 with no feedback connection underscores the importance of feedback mechanism in processing of visual information [171]. However, the connectivity strengths did not increase with task difficulty (<2 % in all cases). This top- down (or feedback) connectivity might regulate the bottom-up process of visual processing [196,197]. These findings show that the involvement of both bottom-up and top-down processes are necessary for successfully evaluating visual stimuli consistent with previous studies [171,177,196-198].

In addition to the modulation of feedforward connectivity by task difficulty, our DCM results also favored the bidirectional connectivity between FFA and PPA. The connectivity between FFA and PPA increased with noise level. This supports the importance of bilateral interactions in visual processing [175,199]. The outperformance of model 8 compared with model 16 favors the hypothesis that the FFA and PPA not only each process its preferred category but also represents the other form of visual objects (for example, non-preferred

category) and their physical properties [34,170,171,198,200,201].

We focused our analysis on category-responsive regions in ventral temporal area of the brain [35,39,170,183,184] and the dlPFC, decision making hub [3,47,83,112,159,174-176,187-189,195,196]. Other brain regions such as Pre-SMA, bilateral inferior parietal lobe (IPL) and bilateral the insular cortex (INS) were also activated by the task. However, we excluded these regions in DCM analysis as these regions are known for supporting cognitive processes such as attention, working memory [202,203]. The peak activation coordinates for pre-SMA obtained in our study are close to the peak activity locations reported in previous studies and was shown be associated with the attention [19,38,204]. The insular activation is known to related with the subjective experience of emotional states and feelings [156]. Similarly, IPL is known to be involved in visual short-term memory [203,205,206]. The choice of a fewer nodes also worked in our favor for the DCM analysis since a large number of nodes in DCM analysis can be computationally expensive and, at times, problematic [207].

Summarizing, we showed how the dynamics of distinct cortical areas contributes to the processing of visual-sensation that leads to perceptual decisions. In relation to our task, evidence supports us to argue that the FFA-PPA-dlPFC network represents a minimal brain circuitry necessary for relaying and integrating competing sensory information, and has a role in decision-making. Future studies using this type of experiment in multisensory domains can lead to uncovering brain functional architectures necessary for more complex perceptual decision-making processes in the brain.

REFERENCES

[1] E. Fehr and C. F. Camerer, Trends Cogn Sci **11**, 419 (2007).

[2] A. G. Sanfey, Science **318**, 598 (2007).

[3] A. G. Sanfey, J. K. Rilling, J. A. Aronson, L. E. Nystrom, and J. D. Cohen, Science **300**, 1755 (2003).

[4] J. K. Rilling and A. G. Sanfey, Annu. Rev. Psychol. **62**, 23 (2011).

[5] E. Fehr and U. Fischbacher, Nature **425**, 785 (2003).

[6] E. Fehr and U. Fischbacher, Evol. Hum. Behav. **25**, 63 (2004).

[7] E. Fehr and K. M. Schmidt, Q. J. Econ. **114**, 817 (1999).

[8] C. F. Camerer, *Behavioral game theory-experiments in strategic interaction* (Princeton Univ. Press, Princeton, NJ., 2003).

[9] W. Guth, R. Schmittberger, and B. Schwarze, J. Econ. Behav. Organ. **3**, 367 (1982).

[10] J. Henrich, R. Boyd, S. Bowles, C. Camerer, E. Fehr, H. Gintis, and R. McElreath, Am. Econ. Rev. **91**, 73 (2001).

[11] E. Fehr and H. Gintis, Annu. Rev. Sociol. **33**, 43 (2007).

[12] E. Xiao and D. Houser, Proc. Natl. Acad. Sci. USA **102**, 7398 (2005).

[13] T. Yamagishi, Y. Horita, H. Takagishi, M. Shinada, S. Tanida, and K. S. Cook, Proc. Natl. Acad. Sci. USA **106**, 11520 (2009).

[14] E. Fehr and U. Fischbacher, Econ. J. **112**, C1 (2002).

[15] P. W. Glimcher, C. F. Camerer, E. Fehr, and R. A. poldrack, *Neuroeconomics - decision making and the brain.* (Elsevier academic press, London, 2009), p.^pp. 538.

[16] D. Houser and K. McCabe, (Emerald insight, London, 2008).

[17] D. Houser and E. Xiao, Econ. Lett. **109**, 20 (2010).

[18] J. I. Gold and M. N. Shadlen, Annu Rev Neurosci **30**, 535 (2007).

[19] H. R. Heekeren, S. Marrett, and L. G. Ungerleider, Nat. Rev. Neurosci. **9**, 467 (2008).

[20] N. U. Dosenbach *et al.*, Proc. Natl. Acad. Sci. USA **104**, 799 (2007).

[21] N. U. Dosenbach *et al.*, Neuron **50**, 799 (2006).

[22] T. C. Ho, S. Brown, and J. T. Serences, J. Neurosci. **29**, 8675 (2009).

[23] R. M. Krebs, C. N. Boehler, K. C. Roberts, A. W. Song, and M. G. Woldorff, Cereb cortex **22**, 607 (2012).

[24] D. Sridharan, D. J. Levitin, and V. Menon, Proc. Natl. Acad. Sci. USA **105**, 12569 (2008).

[25] L. Srinivasan, W. F. Asaad, D. T. Ginat, J. T. Gale, D. D. Dougherty, Z. M. Williams, T. J. Sejnowski, and E. N. Eskandar, PLoS One **8**, e55247 (2013).

[26] V. Venkatraman, A. G. Rosati, A. A. Taren, and S. A. Huettel, J. Neurosci. **29**, 13158 (2009).

[27] K. Wiech, C. S. Lin, K. H. Brodersen, U. Bingel, M. Ploner, and I. Tracey, J. Neurosci. **30**, 16324 (2010).

[28] R. Romo and E. Salinas, Nat. Rev. Neurosci. **4**, 203 (2003).

[29] C. D. Krawczyk, Neurosci. Biobehav. R. **26**, 631 (2002).

[30] M. M. Botvinick, T. S. Braver, D. M. Barch, C. S. Carter, and J. D. Cohen, Psychol. Rev. **108**, 624 (2001).

[31] V. de Lafuente and R. Romo, Nat. Neurosci. **8**, 1698 (2005).

[32] T. Ham, A. Leff, X. de Boissezon, A. Joffe, and D. J. Sharp, J. Neurosci. **33**, 7091 (2013).

[33] A. Ishai, C. F. Schmidt, and P. Boesiger, Brain. Res. Bull. **67**, 87 (2005).

[34] A. Ishai, L. G. Ungerleider, A. Marttin, J. L. Schouten, and J. V. Haxby, Proc. Natl. Acad. Sci. U S A **96**, 9379 (1999).

[35] N. Kanwisher, J. McDermott, and M. M. Chun, J. Neurosci. **17**, 4302 (1997).

[36] W. W. Seeley, V. Menon, A. F. Schatzberg, J. Keller, G. H. Glover, H. Kenna, A. L. Reiss, and M. D. Greicius, J. Neurosci. **27**, 2349 (2007).

[37] W. T. Newsome and E. D. Pare, J. Neurosci. **8**, 2201 (1988).

[38] H. R. Heekeren, P. A. Bandettini, and L. G. Ungerleider, Nature **431**, 859 (2004).

[39] R. Epstein and N. Kanwisher, Nature **392**, 598 (1998).

[40] N. Kanwisher and G. Yovel, Philos. T. Roy. Socl.B. of London. **361**, 2109 (2006).

[41] J. S. Adams, in *Advances in experimental social psychology* edited by L. Berkowitz (New York : Academic, 1965), pp. 267.

[42] E. A. Lind and T. R. Tyler, *The social psychology of procedural justic* (New York: Plenum, 1988).

[43] S. Sprecher, Soc. Psychol. Quart. **49**, 309 (1986).

[44] E. Walster, G. W. Walster, and E. Berscheid, *Equity: Theory and Research.* (New York: Plenum, 1978).

[45] E. Fehr and S. Gachter, Nature **415**, 137 (2002).

[46] S. A. Price and S. F. Brosnan, Soc. Just. Res. **25**, 140 (2012).

[47] D. Knoch, A. Pascual-Leone, K. Meyer, V. Treyer, and E. Fehr, Science **314**, 829 (2006).

[48] G. E. Bolton, E. Katok, and R. Zwick, Int. J. Game Theory **27**, 269 (1998).

[49] G. Tabibnia, A. B. Satpute, and M. D. Lieberman, Psychol Sci **19**, 339 (2008).

[50] D. V. Smith, J. A. Clithero, S. E. Boltuck, and S. A. Huettel, Soc. Cogn. Affect. Neurosci. doi: 10.1093/scan/nsu005 (2014).

[51] J. W. Buckholtz, C. L. Asplund, P. E. Dux, D. H. Zald, J. C. Gore, O. D. Jones, and R. Marois, Neuron **60**, 930 (2008).

[52] G. F. Lowewenstein, L. Thompson, and M. H. Bazerman, J. Pers. Soc. Phychol. **57**, 426 (1989).

[53] J. Dana, R. Weber, and J. X. Kuang, Econ. Theory **33**, 67 (2007).

[54] O. Hikosaka, K. Nakamura, and H. Nakahara, J. Neurophysiol. **95**, 567 (2006).

[55] H. Kim, J. H. Sul, N. Huh, D. Lee, and M. W. Jung, J. Neurosci. **29**, 14701 (2009).

[56] K. Samejima, Y. Ueda, K. Doya, and M. Kimura, Science **310**, 1337 (2005).

[57] M. R. Delgado, H. M. Locke, V. A. Stenger, and J. A. Fiez, Cogn. Affect. Behav. Ne. **3**, 27 (2003).

[58] M. R. Delgado, V. A. Stenger, and J. A. Fiez, Cereb. Cortex **14**, 1022 (2004).

[59] B. Knutson, C. M. Adams, G. W. Fong, and D. Hommer, J. Neurosci. **21RC**, 1 (2001).

[60] C. Martin-Soelch, J. Missimer, K. L. Leenders, and W. Schultz, Eur. J. Neurosci. **18**, 680 (2003).

[61] J. S. Greenberg and R. Cohen, *Equity and justice in social behavior* (Acedemic Press, New York, 1982).

[62] P. McGuire, D. Silbersweig, R. Murray, R. Frackowiak, and D. Frith, Brit. J. Psychiat. **167**, 148 (1996).

[63] P. Verstichel, C. Bourak, V. Font, and G. Crochet, Revue de Neuropsychologie **7**, 281 (1997).

[64] M. Spitzer, U. Fischbacher, B. Herrnberger, G. Gron, and E. Fehr, Neuron **56**, 185 (2007).

[65] B. Ward, Available at http://afni.nimh.nih.gov/pub/dist/doc/manual/AlphaSim.pdf (2000).

[66] M. Brett, J.-L. Anton, R. Valabregue, and J.-B. Poline, Neuroimage (2002).

[67] C. F. Bond and K. Richardson, Psychometrika **69**, 291 (2004).

[68] N. J. Cox, Stata. J. **8**, 413 (2008).

[69] N. C. Silver and W. P. Dunlap, J. Appl. Psychol **72**, 146 (1987).

[70] G. K. Aguirre, E. Zarahn, and M. D'Esposito, NeuroImage **8**, 360 (1998).

[71] D. A. Handwerker, J. M. Ollinger, and M. D'Esposito, NeuroImage **21**, 1639 (2004).

[72] O. David, I. Guillemain, S. Saillet, S. Reyt, C. Deransart, C. Segebarth, and A. Depaulis, PLoS Biol. **6**, 2683 (2008).

[73] A. Roebroeck, E. Formisano, and R. Goebel, NeuroImage **58**, 296 (2011).

[74] P. A. Valdes-Sosa, A. Roebroeck, J. Daunizeau, and K. Friston, NeuroImage **58**, 339 (2011).

[75] G. R. Wu, W. Liao, S. Stramaglia, J. R. Ding, H. Chen, and D. Marinazzo, Med. Image Anal. **17**, 365 (2013).

[76] M. Dhamala, G. Rangarajan, and M. Ding, NeuroImage **41**, 354 (2008).

[77] R. C. Blair and W. Karniski, Psychophysiology **30**, 518 (1993).

[78] A. Brovelli, M. Ding, A. Ledberg, Y. Chen, R. Nakamura, and S. L. Bressler, Proc. Natl. Acad. Sci. U S A **101**, 9849 (2004).

[79] R. S. Blumenfeld, E. M. Nomura, C. Gratton, and M. D'Esposito, Cereb. Cortex **23**, 2457 (2013).

[80] S. Zysset, O. Huber, E. Ferstl, and D. Y. von Cramon, NeuroImage **15**, 983 (2002).

[81] J. Winking and N. Mizer, Evol. Hum. Behav. **34**, 288 (2013).

[82] Y. Zhou, Y. Wang, L. L. Rao, L. Q. Yang, and S. Li, Front. Behav. Neurosci. **8**, 150 (2014).

[83] E. K. Miller and J. D. Cohen, Annu. Rev. Neurosci. **24**, 167 (2001).

[84] D. H. Weissman, A. S. Perkins, and M. G. Woldorff, NeuroImage **40**, 955 (2008).

[85] A. D. Wagner, A. Maril, R. A. Bjork, and D. L. Schacter, NeuroImage **14**, 1337 (2001).

[86] E. K. Miller, Nat Rev Neursci **1**, 59 (2000).

[87] D. J. de Quervain, U. Fischbacher, V. Treyer, M. Schellhammer, U. Schnyder, A. Buck, and E. Fehr, Science **305**, 1254 (2004).

[88] M. R. Delgado, L. E. Nystrom, C. Fissell, D. C. Noll, and J. A. Fiez, J. Neurophysiol. **84**, 3072 (2000).

[89] B. King-Casas, D. Tomlin, C. Anen, C. F. Camerer, S. R. Quartz, and P. R. Montague, Science **308**, 78 (2005).

[90] P. Apicella, T. Ljungberg, E. Scarnati, and W. schultz, Exp. Brain Res. **85**, 491 (1991).

[91] O. Hikosaka, M. Sakamoto, and S. Usui, J. Neurophysiol. **61**, 814 (1989).

[92] W. Schultz, Nat. Rev. Neursci. **1**, 199 (2000).

[93] M. M. Botvinick, J. D. Cohen, and C. S. Carter, Trends Cogn. Sci. **8**, 539 (2004).

[94] R. D. Rogers, N. Ramnani, C. Mackay, J. L. Wilson, P. Jezzard, C. S. Carter, and S. M. Smith, Biol. Psychiatry **55**, 594 (2004).

[95] G. Bush, B. A. Vogt, J. Holmes, A. M. Dale, D. Greve, M. A. Jenike, and B. R. Rosen, Proc. Natl. Acad. Sci. USA **99**, 523 (2002).

[96] Z. M. Williams, G. Bush, S. L. Rauch, G. R. Cosgrove, and E. N. Eskandar, Nat. Neurosci. **7**, 1370 (2004).

[97] M. R. Delgado, Ann. N.Y. Acad. Sci. **1104**, 70 (2007).

[98] C. Camerer, G. Loewenstein, and D. Prelec, J. Econo. Literature. **XLIII**, 9 (2003).

[99] S. Gallagher, Trends. Cogn. Sci. **4**, 14 (2000).

[100] A. Morin, Conscious. Cogn. **18**, 524 (2009).

[101] F. A. Mansouri, K. Tanaka, and M. J. Buckley, Nat. Rev. Neursci **10**, 141 (2009).

[102] D. Passingham and K. Sakai, Curr. Opin. Neurobiol. **14**, 163 (2004).

[103] A. R. Damasio, *Descartes' error: Emotion, reason, and the human brain.* (Harper Collins, New York., 1995).

[104] C. S. Johnson, T. W. Schmitz, T. N. Kawahara-Baccus, T. A. Rowley, A. L. Alexander, J. Lee, and R. J. Davidson, J. Cognitive Neurosci. **17**, 1897 (2005).

[105] T. Baumgartner, D. Knoch, P. Hotz, C. Eisenegger, and E. Fehr, Nat. Neurosci. **14**, 1468 (2011).

[106] N. Gogtay *et al.*, Proc. Natl. Acad. Sci. USA **101**, 8174 (2004).

[107] V. S. Chib, K. Yun, H. Takahashi, and S. Shimojo, Transl. Psychiatry **3**, e268 (2013).

[108] P. E. Bailey, T. Ruffman, and P. G. Rendell, J Gerontol B Psychol. Sci. Soc. Sci. **68**, 356 (2013).

[109] B. King-Casas, C. Shaep, L. Lomax-Bream, T. Lohrenz, P. Fonagy, and P. R. Montague, Science **321**, 806 (2008).

[110] S. Baez *et al.*, PLoS One **8**, e57664 (2013).

[111] J. Grinband, J. Hirsch, and V. P. Ferrera, Neuron **49**, 757 (2006).

[112] E. J. Ploran, S. M. Nelson, K. Velanova, D. I. Donaldson, S. E. Petersen, and M. E. Wheeler, J. Neurosci. **27**, 11912 (2007).

[113] J. R. Binder, E. Liebenthal, E. T. Possing, A. D. Medler, and B. D. Ward, Nat. Neurosci. **7**, 295 (2004).

[114] K. O. Bushara, J. Grafman, and M. Hallett, J. Neurosci. **32**, 300 (2001).

[115] J. W. Lewis, M. S. Beauchamp, and E. DeYoe, Cereb. Cortex **10**, 873 (2000).

[116] J. R. Tregellas, D. B. Davalos, and D. C. Rojas, NeuroImage **32**, 307 (2006).

[117] M. Ploner, M. C. Lee, K. Wiech, U. Bingel, and I. Tracey, Proc. Natl. Acad. Sci. U S A **107**, 355 (2010).

[118] N. Picard and P. L. Strick, Cereb. Cortex **6**, 342 (1996).

[119] Z. M. Williams, G. Bush, S. L. Rauch, G. R. Cosgrove, and E. N. Eskandar, Nat. Neurosci. **7**, 1370 (2004).

[120] M. F. Rushworth, M. E. Walton, S. W. Kennerley, and D. M. Bannerman, Trends. Cogn. Sci. **8**, 410 (2004).

[121] N. Medford and H. D. Critchley, Brain Struct Funct **214**, 535 (2010).

[122] S. Zysset, C. S. Wendt, K. G. Volz, J. Neumann, O. Huber, and D. Y. von Cramon, NeuroImage **31**, 1380 (2006).

[123] P. C. Taylor, A. C. Nobre, and M. F. Rushworth, J. Neurosci. **27**, 11343 (2007).

[124] M. P. van den Heuvel, R. C. Mandl, R. S. Kahn, and H. E. Hulshoff Pol, Hum. Brain. Mapp. **30**, 3127 (2009).

[125] A. Thielscher and L. Pessoa, J. Neurosci. **27**, 2908 (2007).

[126] A. Woolgar, A. Hampshire, R. Thompson, and J. Duncan, J. Neurosci. **31**, 14592 (2011).

[127] A. Shenhav, M. M. Botvinick, and J. D. Cohen, Neuron **79**, 217 (2013).

[128] M. M. Botvinick, T. S. Braver, D. M. Barch, C. S. Carter, and J. D. Cohen, Psychol. Rev. **108**, 624 (2001).

[129] J. Navarra, A. Vatakis, M. Zampini, S. Soto-Faraco, W. Humphreys, and C. Spence, Cognitive. Brain. Res. **25**, 499 (2005).

[130] M. Zampini, D. I. Shore, and C. Spence, Exp. Brain Res. **152**, 198 (2003).

[131] A. Vatakis, J. Navarra, S. Soto-Faraco, and C. Spence, Exp. Brain Res. **181**, 173 (2007).

[132] A. Vatakis and C. Spence, Neurosci. Lett. **393**, 40 (2006).

[133] F. Pons and D. J. Lewkowicz, Acta. Psychol. **149**, 142 (2014).

[134] R. L. J. van Eijk, A. Kohlrausch, J. F. Juola, and S. van de Par, Percept. Psychophys. **70**, 955 (2008).

[135] V. van Wassenhove, K. W. Grant, and D. Poeppel, Neuropsychologia **45**, 598 (2007).

[136] M. Zampini, S. Guest, D. I. Shore, and C. Spence, Percept. Psychophys. **67**, 531 (2005).

[137] S. J. Kiebel, S. Kloppel, N. Weiskopf, and K. J. Friston, NeuroImage **34**, 1487 (2007).

[138] K. J. Friston, L. Holmes, K. J. Worsely, J. B. Poline, C. D. Firth, and R. S. J. Frackowiak, Hum Brain Mapp **2**, 189 (1995).

[139] K. J. Friston, L. Harrison, and W. D. Penny, NeuroImage **19**, 1273 (2003).

[140] W. D. Penny, K. E. Stephan, J. Daunizeau, M. J. Rosa, K. J. Friston, T. M. Schofield, and A. P. Leff, PLoS Comp. Biol. (2010).

[141] M. Ullsperger, H. A. Harsay, J. R. Wessel, and K. R. Ridderinkhof, Brain. Struct. Funct **214**, 629 (2010).

[142] M. M. Mesulam and E. J. Mufson, J. Comp. Neurol. **212**, 23 (1982a).

[143] M. M. Mesulam and E. J. Mufson, J. Comp. Neurol. **212**, 38 (1982b).

[144] B. Pleger, C. C. Ruff, F. Blankenburg, S. Bestmann, K. Wiech, K. E. Stephan, A. Capilla, K. J. Friston, and R. J. Dolan, J. Neurosci. **26**, 12596 (2006).

[145] G. A. Calvert, Cereb cortex **11**, 1110 (2001).

[146] P. Kosillo and A. T. Smith, Brain Struct Funct **214**, 623 (2010).

[147] S. Gluth, J. Rieskamp, and C. Buchel, J. Neurosci. **32**, 10686 (2012).

[148] C. Landmann, S. Dehaene, S. Pappata, A. Jobert, M. Bottlaender, D. Roumenov, and D. Le Bihan, Cereb. Cortex **17**, 749 (2007).

[149] R. J. Morecraft, K. S. Stilwell-Morecraft, P. B. Cipolloni, J. Ge, D. W. McNeal, and D. N. Pandya, Brain Res Bull **87**, 457 (2012).

[150] A. J. Shackman, T. V. Salomons, H. A. Slagter, A. S. Fox, J. J. Winter, and R. J. Davidson, Nat. Rev. Neurosci. **12**, 154 (2011).

[151] D. E. Nee, S. Kastner, and J. W. Brown, NeuroImage **54**, 528 (2011).

[152] M. F. Rushworth, K. A. Hadland, T. Paus, and P. K. Sipila, J. Neurophysiol **78**, 2577 (2002).

[153] V. Menon and L. Q. Uddin, Brain. Struct. Funct. **214**, 655 (2010).

[154] H. D. Critchley, S. Wiens, P. Rotshtein, A. Ohman, and R. J. Dolan, Nat. Neurosci. **7**, 189 (2004).

[155] T. Singer, H. D. Critchley, and K. Preuschoff, Trends. Cogn. Sci. **13**, 334 (2009).

[156] P. Sterzer and A. Kleinschmidt, Brain. Struct. Funct. **214**, 611 (2010).

[157] M. A. Eckert, V. Menon, A. Walczak, J. Ahlstrom, S. Denslow, A. Horwitz, and J. R. Dubno, Hum. Brain. Mapp. **30**, 2530 (2009).

[158] B. M. Adhikari, E. S. Goshorn, B. Lamichhane, and M. Dhamala, Brain. Connect. **3**, 536 (2013).

[159] T. Carlson, M. J. Grol, and F. A. Verstraten, NeuroImage **32**, 892 (2006).

[160] A. Hernandez, V. Nacher, R. Luna, A. Zainos, L. Lemus, M. Alvarez, Y. Vazquez, L. Camarillo, and R. Romo, Neuron **66**, 300 (2010).

[161] B. Lamichhane, B. M. Adhikari, S. F. Brosnan, and M. Dhamala, Brain. Connect. (2014).

[162] E. K. Miller and J. D. Cohen, Annu. Rev. Neurosci. **24**, 167 (2001).

[163] A. Pasupathy and E. K. Miller, Nature **433**, 873 (2005).

[164] D. Badre, R. A. Poldrack, E. J. Pare-Blagoev, R. Z. Insler, and A. D. Wagner, Neuron **47**, 907 (2005).

[165] A. Genovesio and S. Ferraina, J. Neurophysiol. **91**, 2670 (2004).

[166] G. R. Kuperberg, B. M. Lakshmanan, D. N. Greve, and W. C. West, Hum. Brain. Mapp. **29**, 544 (2008).

[167] N. G. Muggleton, C. H. Juan, A. Cowey, and V. Walsh, J. Neurophysiol. **89**, 3340 (2003).

[168] A. Tosoni, G. Galati, G. L. Romani, and M. Corbetta, Nat. Neurosci. **11**, 1446 (2008).

[169] S. Sadaghiani, R. Scheeringa, K. Lehongre, B. Morillon, A. L. Giraud, and A. Kleinschmidt, J. Neurosci. **30**, 10243 (2010).

[170] J. V. Haxby, M. I. Gobbini, M. L. Furey, A. Ishai, J. L. Schouten, and P. Pietrini, Science **293**, 2425 (2001).

[171] J. V. Haxby, A. A. Hoffman, and M. I. Gobbini, Trends. Cogn. Sci. **4**, 223 (2000).

[172] J. V. Haxby, E. A. Hoffman, and M. I. Gobbini, Biol. Psychiatry. **51**, 59 (2002).

[173] G. Avidan and M. Behrmann, Current biology : CB **19**, 1146 (2009).

[174] G. Avidan, U. Hasson, R. Malach, and M. Behrmann, Curr. Biol. **19**, 1146 (2005).

[175] B. Rossion, R. Caldara, M. Seidenberg, A.-M. Schacter, F. Lazeyras, and E. Mayer, Brain. **126**, 2381 (2003).

[176] S. L. Fairhall and A. Ishai, Cereb. cortex **17**, 2400 (2007).

[177] A. Ishai, NeuroImage **40**, 415 (2008).

[178] F. A. W. Wilson, Science **260**, 1955 (1993).

[179] K. H. Britten, M. N. Shadlen, W. T. Newsome, and J. A. Movshon, J. Neurosci. **12**, 4745 (1992).

[180] A. Hernandez, A. Zainos, and R. Romo, Proc. Natl. Acad. Sci. U S A **97**, 6191 (2000).

[181] R. Romo, A. Hernandez, A. Zainos, and E. Salinas, Nature **392**, 387 (1998).

[182] C. D. Salzman, C. M. Murasugi, K. H. Britten, and W. T. Newsome, J.Neurosci **12**, 2331 (1992).

[183] G. K. Aguirre, E. Zarahn, and M. D'Esposito, Neuron **21**, 373 (1998).

[184] P. Vuilleumier, J. L. Armony, J. Driver, and R. J. Dolan, Neuron **30**, 829 (2001).

[185] J. J. Marotta, Neuroreport **12**, 1581 (2001).

[186] C. Schiltz, B. Sorger, R. Caldara, F. Ahmed, E. Mayer, R. Goebel, and B. Rossion, Cereb. cortex **16**, 574 (2006).

[187] J. D. E. Gabrieli, R. A. Poldrack, and J. E. Desmond, Proc. Natl. Acad. Sci. U S A **95**, 906 (1998).

[188] A. Smith, E. Taylor, K. Lidzba, and K. Rubia, NeuroImage **20**, 344 (2003).

[189] M. Bar, R. B. H. Tootell, D. L. Schacter, D. N. Greve, B. Fischl, J. D. Mendola, B. R. Rosen, and A. M. Dale, Neuron **29**, 529 (2001).

[190] G. Rainer and E. K. Miller, Neuron **27**, 179 (2000).

[191] K. J. Friston, L. Harrison, and W. Penny, NeuroImage **19**, 1273 (2003).

[192] A. C. Marreiros, S. J. Kiebel, and K. J. Friston, NeuroImage **39**, 269 (2008).

[193] K. E. Stephan, W. D. Penny, J. Daunizeau, R. J. Moran, and K. J. Friston, NeuroImage **46**, 1004 (2009).

[194] C. L. Leveroni, M. Seidenberg, A. R. Mayer, L. A. Mead, J. R. Binder, and S. M. Rao, J. Neurosci. **20**, 878 (2000).

[195] K. Kveraga, A. S. Ghuman, and M. Bar, Brain. Cogn. **65**, 145 (2007).

[196] A. Mechelli, C. J. Price, K. J. Friston, and A. Ishai, Cereb cortex **14**, 1256 (2004).

[197] J. J. Summerfield, J. Lepsien, D. R. Gitelman, M. M. Mesulam, and A. C. Nobre, Neuron **49**, 905 (2006).

[198] S. Li, S. D. Mayhew, and Z. Kourtzi, Neuron **62**, 441 (2009).

[199] B. Sorger, R. Goebel, C. Schiltz, and B. Rossion, NeuroImage **35**, 836 (2007).

[200] D. J. Freedman, J. Neurosci. **88**, 929 (2002).

[201] R. Kiani, H. Esteky, K. Mirpour, and K. Tanaka, J. Neurophysiol. **97**, 4296 (2007).

[202] H. C. Lau, R. D. Rogers, P. Haggard, and R. E. Passingham, Science **303**, 1208 (2004).

[203] I. R. Olson and M. Berryhill, Neurobiol Learn Mem **91**, 155 (2009).

[204] L. Pessoa, S. Kastner, and L. G. Ungerleider, J. Neurosci. **23**, 3990 (2003).

[205] R. Marois and J. Ivanoff, Trends. Cogn. Sci. **9**, 296 (2005).

[206] R. Marois, D.-J. Yi, and M. M. Chun, Neuron **41**, 465 (2004).

[207] K. E. Stephan, W. D. Penny, R. J. Moran, H. E. den Ouden, J. Daunizeau, and K. J. Friston, NeuroImage **49**, 3099 (2010).